Development, External Validation, and Biomolecular Corroboration of Interoperable Models for Identifying Critically Ill Children at Risk of Neurologic Morbidity

Christopher M. Horvat MD MHA[1,2], Amie J Barda PhD[3], Eddie Perez Claudio BS[4], Alicia K. Au MD MS[1,2], Andrew Bauman PhD[5], Qingyan Li PhD[5], Ruoting Li PhD[5], Neil Munjal MD MS[6], Mark Wainwright MD PhD[5], Tanupat Boonchalermvichien MD[4], Harry Hochheiser PhD[4], Robert S. B. Clark MD[1,2]

1. Department of Critical Care Medicine, University of Pittsburgh, Pittsburgh, PA
2. Safar Center for Resuscitation Research, University of Pittsburgh, Pittsburgh, PA
3. Barda Analytics Consulting LLC, North Royalton, OH
4. Department of Biomedical Informatics, University of Pittsburgh, Pittsburgh, PA
5. Seattle Children's Hospital, Seattle, WA
6. Department of Pediatrics, University of Wisconsin-Madison, Madison, WI

Data Sharing Statement: Data are available for specific use cases with investigator approval.

Funding: NINDS R01NS118716 and NLM 5T15LM007059-38

Corresponding Author: Christopher Horvat, MD MHA, UPMC Children's Hospital of Pittsburgh, 4401 Penn Ave, Pittsburgh, PA 15224; Christopher.horvat@chp.edu; Ph (412) 692-5298.

Key Points

Question Can interoperable models for predicting neurological deterioration in critically ill children be developed, correlated with serum-based brain-derived biomarkers, and validated at an external site?

Findings A development site model demonstrated an area under the receiver operating characteristics curve (AUROC) of 0.82 and a number needed to alert (NNA) of 2. Predictions correlated with levels of glial fibrillary acidic protein in a subset of children. A generalizable model demonstrated an AUROC of 0.81 and NNA of 4 at the validation site.

Meaning Well performing prediction models coupled with brain biomarkers may help to identify critically ill children at risk for acquired neurological morbidity.

Abstract

Importance Declining mortality in the field of pediatric critical care medicine has shifted practicing clinicians' attention to preserving patients' neurodevelopmental potential as a main objective. Earlier identification of critically ill children at risk for incurring neurologic morbidity would facilitate heightened surveillance that could lead to timelier clinical detection, earlier interventions, and preserved neurodevelopmental trajectory.

Objective Develop machine-learning models for identifying acquired neurologic morbidity while hospitalized with critical illness and assess correlation with contemporary serum-based, brain injury-derived biomarkers.

Design Retrospective cohort study.

Setting Two large, quaternary children's hospitals.

Exposures Critical illness.

Main Outcomes and Measures The outcome was neurologic morbidity, defined according to a computable, composite definition at the development site or an order for neurocritical care consultation at the validation site. Models were developed using varying time windows for temporal feature engineering and varying censored time horizons prior to identified neurologic morbidity. Optimal models were selected based on F1 scores, cohort sizes, calibration, and data availability for eventual deployment. A generalizable created at the development site was assessed at an external validation site and optimized with spline recalibration. Correlation was assessed between development site model predictions and measurements of brain biomarkers from a convenience cohort.

Results After exclusions there were 14,222-25,171 encounters from 2010-2022 in the development site cohorts and 6,280-6,373 from 2018-2021 in the validation site cohort. At the development site, an extreme gradient boosted model (XGBoost) with a 12-hour time horizon and 48-hour feature engineering window had an F1-score of 0.54, area under the receiver operating characteristics curve (AUROC) of 0.82, and a number needed to alert (NNA) of 2. A generalizable XGBoost model with a 24-hour time horizon and 48-hour feature engineering window demonstrated an F1-score of 0.37, AUROC of 0.81, AUPRC of 0.51, and NNA of 4 at the validation site. After recalibration at the validation site, the Brier score was 0.04. Serum levels of the brain injury biomarker glial fibrillary acidic protein measurements significantly correlated with model output (r_s=0.34; *P*=0.007).

Conclusions and Relevance We demonstrate a well-performing ensemble of models for predicting neurologic morbidity in children with biomolecular corroboration. Prospective assessment and refinement of biomarker-coupled risk models in pediatric critical illness is warranted.

Introduction

An estimated 340,000 children are hospitalized with critical illness every year in the United States and brain injury has been cited as the proximate cause of death in approximately 90% of previously healthy children who do not survive their intensive care admission.[1,2] Of children who survive critical illness, acquired neurologic morbidity can have long-lasting implications which range from mild impairments in cognition to profound debilitation. Declining mortality in the field of pediatric critical care has led to increased attention to the longer-term functional outcomes of children who survive an intensive care admission.[3]

Granular, time-series data harbored by the electronic health record (EHR) offer a rich training ground for probabilistic models of important patient outcomes. Implementing well-performing models as clinical decision support (CDS) systems is a promising approach for improving outcomes related to many different conditions and situations, though there are currently no established tools for identifying children at risk for new brain injury.[4–7] Recently enacted federal mandates in the United States of America (USA) are promoting the development of EHRs that facilitate the deployment of interoperable decision support tools built to leverage a core dataset.[8]

The main objective of the present work was to construct and externally validate predictive models to support the identification of critically ill children at high risk for acquired neurologic morbidity, as a first step towards the development of a decision support tool that might be used to forewarn of neurologic morbidity amongst critically ill children, as well as to aid in the enrichment of prospective trials examining strategies to mitigate the risk of brain injury during pediatric critical illness. A second objective was to corroborate the biological underpinnings of the developed prediction models by assessing correlation with novel, brain-

derived, serum-based biomarkers of brain injury obtained from a diagnostically diverse cohort of critically ill children.

Methods

Study Sites

Model development used data from all encounters to a quaternary pediatric intensive care unit (PICU) in a large, freestanding children's hospital between January 1, 2010 and December 31, 2022. The development site PICU serves a region of approximately 5 million people, encompassing Western Pennsylvania and bordering states, and is a level 1 pediatric trauma center. External model validation occurred using data from encounters admitted between January 1, 2018 and December 31, 2023 to a quaternary PICU in a large, freestanding children's hospital that serves as a referral center for the 5-state region of Washington, Wyoming, Alaska, Montana, and Idaho. Approval was granted by the institutional review boards of the University of Pittsburgh (Institutional Review Board [IRB] #17030743) and Seattle Children's Hospital (IRB #STUDY00001374). Findings are reported according to the Transparent Reporting of a Multivariable Prediction Model for Individual Prognosis or Diagnosis (TRIPOD) statement (**Supplemental Table 1**).

Model Development Frameworks

Conceptualization of the model adhered to the Littenberg framework for the development of clinical decision support tools, which considers the clinical and technical plausibility of the tool, as well as the process outcomes, patient outcomes, and eventual societal outcomes addressed by the tool (**Supplemental Table 2**).[9] The first 5 steps of the cross-industry standard process for data modeling (CRISP-DM) framework were followed for model design. CRISP-DM outlines

six steps for data science projects that include 1) understanding the use case; 2) understanding the data; 3) data curation; 4) model development; 5) model evaluation; and 6) model deployment.[10]

Model Development Approach

Model development proceeded in 2 phases: 1) Development of models for use locally at the development site; 2) Development of generalizable models with external validation. The outcome of neurologic morbidity was defined using structured EHR data surrogates based on each study site's clinical and electronic workflows. At the development site, the outcome was a previously validated, computable, composite definition of neurologic morbidity that incorporated orders for electroencephalography (EEG), brain computed tomography (CT), brain magnetic resonance imaging (MRI), or indicators of treated delirium within 72-hours of one another (**Supplemental Table 3**).[11] This outcome has also been validated in a separate cohort of children with sepsis.[12] At the validation site, orders for a neurocritical care service consultation were deemed to be the most reliable surrogate for neurologic morbidity during an episode of critical illness. Data for control cases (hospitalized children who did not meet the definition of a neurologic morbidity) were collected from a random period during the encounter with preference to a window following the first PICU admission.

Candidate data elements for model construction were selected based on clinical expertise and with attention to the United States Core Data for Interoperability (USCDI) requirements to facilitate eventual, interoperable deployment (**Supplemental Tables 4 and 5**).[13] A 'Biodigital Rapid Alert to Identify Neurologic morbidity, A-I bundle (BRAIN A-I)' standard clinical vocabulary value set was filed with the National Library of Medicine's Value Set Authority Center.[14] Features were engineered with the dual aims of representing the temporality of the data

while also preserving clinical interpretability of the features, using methods previously reported.[15] Features were then discretized, or categorized into information bins, with missingness encoded as a feature. In addition to preserving possible information associated with missingness, discretization was performed to reduce the influence of outlier data, represent data nonlinearity in linear modeling processes such as logistic regression, further mitigate overfitting, and preserve clinical interpretability of the features. Additional details of data curation and model development are in the **Supplemental Model Methods**. **Supplemental Figure 4** summarizes model construction at the development site and evaluation at the external validation site. At the development site, data were queried from an Oracle (Oracle Corp, Austin, TX) data warehouse containing a subset of transformed tables from the Cerner Millennium database (Oracle Cerner, Kansas City, MO). The model was developed and assessed using Python (version [v]3.10.11), Jupyter (v1.0.0), and the packages *Pandas* (v1.5.3), *Numpy* (v1.25.0), *Matplotlib* (v3.71.1), *Sklearn* (v1.1.1), *XGBoost* (v1.7.3), Seaborn (v0.11.2), SHAP (v0.41.0), and *tqdm* (v4.65.0).

Biomolecular Corroboration of the Model at the Development Site

Model predictions were compared to measured levels of 6 serum-based, brain-derived biomarkers of brain injury obtained from a previously assembled convenience cohort of 101 children hospitalized between 2012-2014 (IRB #19040172). The biomarkers were ubiquitin C-terminal hydrolase-L1 (UCH-L1), glial fibrillary acidic protein (GFAP), myelin basic protein (MBP), neuron-specific enolase (NSE), S100 calcium binding protein B (S100B), and spectrin breakdown product 150 (SBDP150). After prospective consent from a legal guardian, biomarker levels were collected for up to 7 consecutive days from critically ill children with preexisting central venous catheters or arterial catheters. Details of the assays are provided in the **Supplemental Biomarker Methods**. Maximum values of each biomarker for each encounter

were assessed for correlation with the predicted probability of neurologic deterioration for that encounter. Patients were determined to have a neurologic complication by chart review if it occurred no more than 7 days after the last date a biomarker was collected.

Model Selection and Statistical Analysis

The top-performing model was selected based on F1 score, considering a clinically actionable time horizon, as well as the volume of available training data for feature engineering. Models with <0.15 difference in F1 scores were then compared both by visual inspection of calibration plots and Brier scores. Additional Fβ thresholds of 0.5, 2, and 3 were secondarily evaluated to identify whether there were any substantial differences in the optimal classifier based on the relative weight of recall compared to precision. Statistical performances of the top-performing models were evaluated at varied model outputs ranging from 0.025 to 0.9. Spline regression was performed on top-performing models to improve calibration. Normally distributed continuous data are presented as means and 95% confidence intervals, nonparametric continuous data are presented as medians with interquartile ranges (IQRs), and categorical data are presented as counts with corresponding proportions. Model discrimination was compared to the discrimination of the last Glasgow coma scale (GCS) score prior to the censored time horizon using DeLong's method. For the biomolecular corroboration analysis, Spearman's rank-order correlation was assessed between a chart-adjudicated neurologic morbidity outcome and the composite neurologic morbidity outcome, as well as between the probability output of top-performing models and the composite neurologic morbidity outcome. Correlation was then assessed between biomarker levels and the probability output of the top-performing models. Notched boxplots with overlying violin plots were constructed for significantly correlated biomarkers by dichotomizing predicted neurologic morbidity according to whether the

probability was <0.5 or ≥0.5. The distributions of biomarker measurements were normalized for plotting using log transformation and significance testing was assessed using an independent *t* test. An $\alpha < 0.05$ is considered significant. Statistical analyses not performed in Python were performed in R version 4.3.1 (R Foundation, Vienna, Austria).

Results

Development Site Models Performance

There were 32,702 encounters with a PICU stay. After exclusions, cohort sizes ranged from 14,222-25,171 encounters, with 18,568 encounters in the final model cohort (**Supplemental Table 8; Figure 1A**). Patients were slightly older, received less mechanical ventilation, and less sedative-analgesic medications in the final test dataset compared to the training and validation datasets (**Table 1**). The final models evaluated in the test dataset was the extreme gradient boosting (XGBoost) model with a 12-hour time horizon and 48-hour feature window. This model was determined by investigator agreement to be a reasonable balance of favorable F1 scores, calibration as assessed by a Brier score, visual inspection of the calibration plot, clinically actionable time horizon, and sufficient cohort size for the training, validation, and test datasets. Complete development site model performance characteristics, 1 for each of the combinations of a 6, 12, and 24-hour censored time horizons and 24, 48, and 72-hour feature windows selected based on F1 score, are detailed in **Supplemental Table 9**. Each approach generated 605 features prior to information gain feature selection. The F1 scores are reported in **Supplemental Tables 10A and 10B**. Additional Fβ scores largely agreed with the model assessments provided by F1 scores and are presented in **Supplemental Table 11A-C**.

The final model contained 352 features and had a number needed to alert (NNA) of 2 when considering a model prediction of greater than or equal to 0.5 as positive. At a model prediction threshold of 0.025 in the test dataset, sensitivity increased to 0.86 and NAA was 4. Statistical performance of the top-performing validation models and final test model at a range of output thresholds are in **Supplemental Table 12A and 12B** and **Supplemental Figure 5**. All development site models had a NNA of 2-3 at this prediction threshold. In the test dataset the final model had a sensitivity of 0.47 (range for all models in the validation dataset [range] 0.24-0.63), specificity of 0.98 (range 0.96-0.99), AUPRC 0.68 (range 0.39-0.78), and AUROC of 0.89 (range 0.80-0.87). The final model had significantly greater discrimination compared to the last GCS AUROC of 0.72 obtained prior to the censored time horizon, $P<0.001$. Calibration plots of models with comparable performance based on F1-scores are displayed in **Supplemental Figure 6**. The top 10 features of the final model are displayed in **Supplemental Figure 7**. Average hourly scores for cases and controls for the 12 hours preceding and 4 hours following an outcome event are displayed in **Figure 2**.

Biomolecular Corroboration at the Development Site

Of the 101 patients with available brain-derived biomarkers measured, 64 also had model predictions for the 12-hour time horizon and 48-hour feature window models. Chart-adjudicated neuromorbidity within 7 days of last biomarker collection was significantly correlated with the composite neurologic morbidity outcome, $r_s=0.38$ ($P=0.002$). The extreme gradient boosting model was significantly correlated with the composite neurologic morbidity outcome, $r_s=0.80$ ($P<0.001$). The logistic regression model had an F1 score that was nearly identical to the extreme gradient boosting model and was also significantly correlated with the composite neurologic

morbidity outcome, r_s=0.55 (*P*<0.001). Extreme gradient boosting predictions were significantly correlated with maximum GFAP measurements, r_s=0.34 (*P*=0.007) (**Figure 3**).

Generalizable Model Performance

Cohort ascertainment for the generalizable model is reported for the 24-hour time horizon and 48-hour feature window model at the development site in **Supplemental Table 8** and for the validation site in **Supplemental Table 13**. The generalizable model performance at the development and validation sites is reported in **Table 2**. Performance was comparable to earlier 24-hour time horizon 48-hour feature window models at the development. As the XGBoost and logistic regression models performed comparably, both were assessed at the validation site. There were 6,825 encounters in the external validation site final cohort (387 cases and 6,438 controls). As assessed by an F1 score of 0.37 at a threshold of 0.5, the top performing model was the XGBoost model, with an external validation AUROC of 0.81, AUPRC of 0.51, and an NNA of 4. Model performance characteristics across varied thresholds are displayed in **Supplemental Table 14** and **Supplemental Figure 8**. Calibration was again excellent at the development site, initially poor at the external validation site, then substantially improved after spline recalibration at the validation site (**Supplemental Figure 9**). Feature importance analysis for the generalizable model was similar between the development and validation sites (**Supplemental Figure 10**). All models outperformed the GCS, *P*<0.001.

Discussion

In this study, we constructed well-performing models for predicting neurologic morbidity among critically ill children using EHR data from 2 large children's hospitals. These models were trained using more than 600 features engineered to capture nonlinear relationships between

predictors and the outcome. The top performing model at the development site had 352 features and a NNA of 2, suggesting the utility of incorporating more features than can be accommodated by traditional, manually-tabulated clinical decision rules. A generalizable model demonstrated robust performance at both the development site and the external validation site. All models outperformed the GCS, supporting machine-learning-based methods to facilitate clinical activities including identification of high-risk patients for clinical intervention and for identifying an enriched population for enrollment in clinical trials.[16] By largely adhering to data elements prioritized by USCDI, the developed models have a clearer path to implementation in modern informatics architectures capable of data transfer using standard clinical vocabularies and the fast healthcare interoperability resources (FHIR) standard.[17] The generalizable model relies on 41 variables, 37 of which are included in USCDI versions 1 or 2 and are therefore expected to ease eventual work associated with deployment.

Many predictive models are constructed utilizing a snapshot of information from a discrete moment in time.[18,19] For predictive models to more completely leverage the content of the EHR, the temporality of data must be incorporated into model features. The performance of the present models was likely bolstered by incorporating features engineered using vector space representations of patient state, resulting in performance metrics that surpass those of other commonly used critical care risk models.[15] The Simplified Acute Physiology Score, a commonly used mortality prediction tool for critically ill adults, has reported AUPRCs between 0.2-0.3 for in-hospital and 30-day mortality.[20] The sequential organ failure assessment (SOFA), quick SOFA, and systemic inflammatory response syndrome criteria have reported AUPRCs of 0.06, 0.1, and 0.09 predicting mortality at the time of sepsis onset, respectively.[21] By comparison, our model ensemble had AUPRCs ranging from 0.39-0.78 at the development site and 0.2-0.42 at the

validation site. We undertook the present work with an expectation that identification of impending neurologic deterioration requires examination of contextual elements of care and more subtle vital sign and laboratory signatures which may serve as a harbinger of unfavorable trajectory.

Correlation between a top-performing model and measurements of GFAP from a convenience cohort is compatible with our previous investigations of brain biomarkers in critically ill children.[22] GFAP is found in astrocytes and plays a role responding to central nervous system injuries and related neurodegeneration.[23] GFAP measurements from our convenience cohort were obtained for the first 7 days of the PICU stay and may have been obtained remote from an incurred brain injury, including one detected by the composite neurologic morbidity outcome. Notably, our composite neurologic morbidity outcome was significantly correlated with chart-adjudicated neurologic morbidity and an XGBoost model was significantly associated with GFAP levels. Most extensively studied in the context of traumatic brain injury, a growing body of evidence suggest GFAP may be useful to identify more subtle insults to the central nervous system, and that the ability to measure GFAP in the bloodstream in non-traumatic diseases might relate to its dispersion into the bloodstream via recently discovered glymphatic pathways.[24,25] Our models may prove useful both to determine for which patients a GFAP level should be obtained, as well as coupled with the GFAP measurements to bolster model performance.

This work has some important limitations. Use of a composite definition of neurological morbidity intrinsically omits occult neurological morbidities that did not trigger clinical action and represents a source of potential bias in model development. While the computable composite definition of neurologic morbidity used in the present study has previously demonstrated high

specificity, the modest sensitivity of the definition suggests that the present models may miss neurologic morbidities that do not warrant inpatient imaging, EEG, a mental health assessment or a medication directed at psychosis or delirium. This limitation, however, can be mitigated by assessing performance characteristics, including varied Fβ scores or sensitivities at different output thresholds, according to context and adjusting the model actionable threshold in a manner tailored to the clinical environment in which it is deployed. Moreover, while performance was robust at an external validation site relative to other established risk scores, statistical metrics did deteriorate compared to those observed in the test dataset at the development site. Notably, the GCS also had a lower AUROC at the validation site compared to the GCS AUROC at the development site, suggesting that the choice of neurocritical care consult as an outcome influenced the models' performance characteristics.

In conclusion, we developed well-performing models for predicting children with critical illness at risk for neurologic morbidity. A flexible, distributed strategy for model development in partnership with an external validation site demonstrated the utility of adapting to varied informatics infrastructures and EHR deployments to generate well-performing predictive models for a common clinical goal. A generalizable model demonstrated robust performance in external validation. Prospective, multi-site assessment of a generalizable model coupled with brain-based biomarkers is warranted to assess the combined utility for identifying patients at high-risk for incurred neurologic morbidity and evaluating interventions to improve outcomes in this population.

Acknowledgements

We would like to posthumously thank Dr. Ron Hayes (Banyan Biomarkers) for brain biomarker measurements; Dr. Pat Kochanek for helpful guidance; Dr. Henry Ogoe for helping to

run an early version of the pipeline at UPMC Children's Hospital of Pittsburgh; Mrs. Nassima Bouhenni for her initial efforts updating code; Mr. Dan Ricketts for his assistance setting up and maintaining virtual machines used for the final analyses; and Mr. Thomas Mathie for his assistance querying EHR data. United States Patent Application No. 17/760,558 and International Patent Application PCT/US2020/061985 have been filed related to this work.

References

1 Au AK, Carcillo JA, Clark RSB, Bell MJ. Brain injuries and neurological system failure are the most common proximate causes of death in children admitted to a pediatric intensive care unit. *Pediatr Crit Care Med* 2011; **12**: 566–71.

2 Bell JL, Saenz L, Domnina Y, *et al.* Acute Neurologic Injury in Children Admitted to the Cardiac Intensive Care Unit. *Ann Thorac Surg* 2019; **107**: 1831–7.

3 Pollack MM, Holubkov R, Funai T, *et al.* Simultaneous Prediction of New Morbidity, Mortality, and Survival Without New Morbidity From Pediatric Intensive Care: A New Paradigm for Outcomes Assessment. *Crit Care Med* 2015; **43**: 1699–709.

4 Sepanski RJ, Godambe SA, Mangum CD, Bovat CS, Zaritsky AL, Shah SH. Designing a pediatric severe sepsis screening tool. *Front Pediatr* 2014; **2**: 56.

5 Schlapbach LJ, MacLaren G, Festa M, *et al.* Prediction of pediatric sepsis mortality within 1 h of intensive care admission. *Intensive Care Med* 2017; **43**: 1085–96.

6 Ruiz VM, Saenz L, Lopez-Magallon A, *et al.* Early prediction of critical events for infants with single-ventricle physiology in critical care using routinely collected data. *J Thorac Cardiovasc Surg* 2019; **158**: 234-243.e3.

7 Sutherland SM. Electronic Health Record-Enabled Big-Data Approaches to Nephrotoxin-Associated Acute Kidney Injury Risk Prediction. *Pharmacotherapy* 2018; **38**: 804–12.

8 21st Century Cures Act: Interoperability, Information Blocking, and the ONC Health IT Certification Program. Federal Register. 2020; published online May 1. https://www.federalregister.gov/documents/2020/05/01/2020-07419/21st-century-cures-act-interoperability-information-blocking-and-the-onc-health-it-certification (accessed Nov 26, 2022).

9 Littenberg B. Technology assessment in medicine. *Academic Medicine* 1992; **67**: 424–8.

10 Schröer C, Kruse F, Gómez JM. A Systematic Literature Review on Applying CRISP-DM Process Model. *Procedia Computer Science* 2021; **181**: 526–34.

11 Alcamo AM, Clark RSB, Au AK, *et al.* Factors Associated With Neurobehavioral Complications in Pediatric Abdominal Organ Transplant Recipients Identified Using Computable Composite Definitions. *Pediatr Crit Care Med* 2020; **21**: 804–10.

12 Alcamo AM, Barren GJ, Becker AE, *et al.* Validation of a Computational Phenotype to Identify Acute Brain Dysfunction in Pediatric Sepsis. *Pediatr Crit Care Med* 2022; **23**: 1027–36.

13 United States Core Data for Interoperability (USCDI). https://www.healthit.gov/isa/united-states-core-data-interoperability-uscdi (accessed Aug 8, 2022).

14 Value Set Authority Center. https://vsac.nlm.nih.gov/ (accessed Nov 6, 2023).

15 Hauskrecht M, Batal I, Valko M, Visweswaran S, Cooper GF, Clermont G. Outlier detection for patient monitoring and alerting. *Journal of Biomedical Informatics* 2013; **46**: 47–55.

16 Harrer S, Shah P, Antony B, Hu J. Artificial Intelligence for Clinical Trial Design. *Trends in Pharmacological Sciences* 2019; **40**: 577–91.

17 Shareable Clinical Decision Support. http://www.healthit.gov/isa/shareable-clinical-decision-support (accessed Nov 7, 2023).

Tables and Titles

Table 1. Demographic characteristics of the entire cohort and the parsed training, validation, and final test datasets at the development site and the entire cohort, training, and validation datasets, as well as the generalizable model validation dataset at the external validation site.

Table 2. Performance of the generalizable model at the development and external validation sites.

Supplemental Table 1. TRIPOD checklist.

Supplemental Table 2. Littenberg framework for the assessment of medical technology as applied to BRAIN A-I.

Supplemental Table 3. Data curation steps for individual data elements for the BRAIN AI outcome.

Supplemental Table 4. Data curation steps for individual data elements for BRAIN A-I.

Supplemental Table 5. Standard vocabulary crosswalk for BRAIN-AI components.

Supplemental Table 6. Predictive performance of the XGBoost model with a 12-hour censor horizon and 48-hour feature window in the test dataset, after manual tuning, and after Bayesian tuning.

Supplemental Table 7. Predictive performance of the XGBoost model with a 12-hour censor horizon and 48-hour feature window in the validation dataset, after manual tuning, and after Bayesian tuning.

Supplemental Table 8. Cohort ascertainment and exclusions for varied censored time horizons and feature windows at the development site.

Supplemental Table 9. Performance of the optimal models in the validation dataset at the development and validation sites.

Supplemental Table 10 A) F1 scores of top performing models in the development site validation dataset. **B)** F1 scores of top performing models in the validation site test dataset.

Supplemental Table 11 A) F_β (β=2) scores of top performing models in the development site validation dataset; **B**) F_β (β=3) scores of top performing models in the development site validation dataset; **C**) F_β (β=0.5) scores of top performing models in the development site validation dataset.

Supplemental Table 12 A) Statistical performance of the 12-hour time horizon, 48-hour feature window XGBoost and logistic regression models over a range of score thresholds in the development site validation dataset; **B**) Statistical performance of the 12-hour time horizon, 48-hour feature window XGBoost model over a range of score thresholds in the development site test dataset.

Supplemental Table 13. Cohort ascertainment and exclusions for varied feature windows for the validation site.

Supplemental Table 14 A) Statistical performance of the extreme gradient boosting (XGBoost) and logistic regression generalizable models at the development site across varied output thresholds. **B)** Statistical performance of the extreme gradient boosting (XGBoost) and logistic regression generalizable models at the external validation site across varied output thresholds.

Figures and Legends

Figure 1. Cohort ascertainment for the final model at the development site, which included features engineered using 48 hours of preceding data and censoring 12-hours prior to the event for cases. Initial model development and validation proceeded using data from 2010-2019. The model was tested using data from 2020-2022. Abbreviations: LASSO, least absolute shrinkage and selection operator; PICU, pediatric intensive care unit; XGBoost, extreme gradient boosting.

Figure 2. Average hourly scores in the test dataset (encounters with a PICU stay in the year 2020 – 2022) for varied censored time horizon windows for the extreme gradient boosted model developed using a 12-hour time horizon and 48-hour feature window. The red dots are the average hourly scores 12 hours prior to an event and 4 hours after an event for the case encounters (encounters with an identified neurologic morbidity) and the shaded red region represents the 95% confidence interval. The black dots are the average hourly scores for the control encounters (encounters without an identified neurological morbidity). Confidence intervals for the control encounters are not discernable in the figure due to the large cohort size. The size of the dots is proportionate to the cohort size at that timepoint.

Figure 3. Log-transformed maximum GFAP measurements for a convenience cohort of 64 patients, stratified by predicted neurologic morbidity using the 12-hour time horizon 48-hour feature window extreme gradient boosting model. Abbreviations: GFAP, glial fibrillary acidic protein; mL, milliliter; pg, picogram.

Supplemental Figure 1. A representation of the time window and censor horizons used to define cases and controls as part of the development, validation, and test cohorts. The blue boxes in the top, ‘Cases’ box identify a time window that is also demarcated by a horizontal, gold, bidirectional arrow, the horizontal black lines represent length of stay for individual encounters, the vertical black line represents the occurrence of the neurological morbidity outcome, and the gold, horizontal, bidirectional arrow indicates the censor horizon, or period of time that data were not incorporated into the model. In the bottom, ‘Controls’ box, the blue boxes indicate the time window of data used for each stage of model development and evaluation.

Supplemental Figure 2. Data cleaning and feature engineering process.

Supplemental Figure 3. A representation of the feature engineering for continuous biomarker measurements. Temporal information is represented as a variety of summary measurements for discrete windows of time. Feature windows of 24-hours, 48-hours, and 72-hours are displayed in the figure. The models at the development site were trained with 6-hour, 12-hour, and 24-hour censored time horizons, with 12-hour and 24-hour horizons demonstrated in the figure. Definitions and related examples for a 24-hour window of data prior to the censor period are displayed in the table. Abbreviations: h, hours.

Supplemental Figure 4. The process of BRAIN A-I model development and external validation. Curated data at the development site were divided into a train cohort, validation cohort, and 2-years of holdout test data. The curated data were used to generate synthetic data with comparable single variable statistical distributions. The synthetic data were then distributed to

the external validation site with model training code, facilitating local data curation by providing the necessary details of data structure. Finally, the working BRAIN A-I pipeline was applied to real-world data at the external validation site, applied separate training and validation datasets. Abbreviations: BRAIN A-I, Biodigital Rapid Alert to Identify Neuromorbidity A-I Bundle; Dev. Site, Development Site; Valid. Site, Validation Site.

Supplemental Figure 5. Plots the key statistical performance metrics sensitivity (gold line), positive predictive value (PPV, red line), F1 score (blue line), and F2 score (green line) with metric values on the y-axis and model output thresholds on the x-axis for A) the logistic regression model with a 12-hour time horizon and 48-hour feature window in the development site validation dataset; B) the extreme gradient boosting model with a 12-hour time horizon and 48-hour feature window in the development site validation dataset; and C) the extreme gradient boosting model with a 12-hour time horizon and 48-hour feature window in the development site test dataset.

Supplemental Figure 6. Calibration plots and associated Brier scores for the top performing models for varied time horizons and features windows in the validation dataset. A) 6-hour time horizon and 24-hour feature window; B) 6-hour time horizon and 48-hour feature window; C) 6-hour time horizon and 72-hour feature window; D) 12-hour time horizon and 24-hour feature window; E) 12-hour time horizon and 48-hour feature window; F) 12-hour time horizon and 72-hour feature window; G) 24-hour time horizon and 24-hour feature window; H) 24-hour time horizon and 48-hour feature window; I) 24-hour time horizon and 72-hour feature window. Abbreviations: LR, logistic regression; XGB, extreme gradient boosted.

Supplemental Figure 7. Top 10 biomarker feature categories based on Shap values for the 12-hour time horizon 48-hour feature window XGBoost model from the development site. Each category contains several features, e.g. Temperature contains maximum temperature, minimum temperature, average temperature, etc. The blue bars represent the sum of the mean Shap values for each category. Abbreviations: biomrkrs, biomarkers.

Supplemental Figure 8. Plots the key statistical performance metrics sensitivity (gold line), positive predictive value (PPV, red line), F1 score (blue line), and F2 score (green line) with metric values on the y-axis and model output thresholds on the x-axis for the generalizable A) logistic regression model in the development site test dataset; B) extreme gradient boosting model in the development site test data set; C) logistic regression model in the external validation dataset; D) extreme gradient boosting model in the external validation site dataset.

Supplemental Figure 9. Calibration plots for the generalizable model in the **A**) development site test dataset and **B**) the external validation site dataset.

Supplemental Figure 10. Feature importance analysis for the generalizable model in the **A**) development site test dataset and **B**) external validation site dataset.

Additional Materials

Supplemental Model Methods

Supplemental Biomarker Methods

Table 1. Demographic characteristics of the entire cohort and the parsed training, validation, and final test datasets at the development site and the entire cohort, training, and validation datasets, as well as the generalizable model validation dataset at the external validation site.

	Development Site				Validation Site
Characteristic	**Entire Cohort**	**Training Dataset**	**Validation Dataset**	**Final Test Dataset**	**Generalizable Model Validation Dataset**
	N = 18,568	**n = 10,744**	**n = 3,582**	**n = 4,242**	**N = 6,825**
Age (months), median (IQR)	70 (18, 161)	67 (18, 158)	68.5 (18, 160)	77 (19, 167)	96 (18,171)
Female, n (%)	8,325 (45)	4,748 (44)	1,593 (44)	1,984 (47)	3,159 (46)
Glasgow Coma Scale Score, median (IQR)*	15 (12, 15)	15 (11, 15)	15 (11, 15)	15 (14, 15)	14 (14,15)
Mechanical Ventilation, n (%)	5,352 (29)	3,322 (31)	1,143 (32)	887 (21)	1,948(29)
Endotracheal Tube, n (%)	1,759 (9)	1,142 (11)	370 (10)	247 (6)	1,283 (19)
Vasoactive Medication, n (%)**	720 (4)	393 (4)	148 (4)	179 (4)	221 (3)
Sedative-Analgesic Medication, n (%)***	4,660 (25)	2,948 (27)	987 (27)	727 (17)	1,930 (28)

*The last recorded Glasgow coma scale score for the encounter prior to the censored time horizon
**Vasoactive medications include dobutamine, dopamine, epinephrine, norepinephrine, or milrinone
***Sedative-analgesic medications include fentanyl, hydromorphone, midazolam, or morphine
Abbreviations: IQR, interquartile range

Table 2. Performance of the generalizable model at the development and external validation sites.

	Development Site						Validation Site	
Dataset	**Development**		**Validation**		**Test**		**External Validation**	
Encounters (Cases/Controls), N	10,457 (1,095/9,362)		3,486 (365/3,121)		4,152 (398/3,754)		6,825 (387/6,438)	
Model	XGB	LR	XGB	LR	XGB	LR	XGB	LR
Feature Selection	IG	IG	IG	IG	IG	IG	IG	IG
AUROC	1.00	0.90	0.81	0.81	0.87	0.86	0.81	0.82
AUPRC	0.99	0.71	0.52	0.54	0.62	0.61	0.51	0.48
PPV	1.00	0.84	0.67	0.69	0.82	0.80	0.26	0.18
NPV	0.99	0.94	0.93	0.93	0.94	0.94	0.97	0.98
Sensitivity	0.91	0.47	0.35	0.41	0.35	0.38	0.61	0.70
Specificity	1.00	0.99	0.98	0.98	0.99	0.99	0.90	0.81
F1 score	0.95	0.61	0.46	0.51	0.49	0.52	0.37	0.29
F2 score	0.92	0.52	0.39	0.45	0.39	0.43	0.48	0.45
F3 score	0.92	0.50	0.37	0.43	0.37	0.41	0.54	0.55
F0.5 score	0.98	0.73	0.57	0.60	0.65	0.66	0.30	0.22

Abbreviations: AUROC, area under the receiver operating characteristics curve; AUPRC, area under the precision recall curve; CFS, correlation-based feature selection; IG, information gain; LR, logistic regression; NB, naïve Bayes; NPV, negative predictive value; PPV, positive predictive value; XGB, XGBoost (extreme gradient boosting)

TRIPOD Checklist: Prediction Model Development

Section/Topic	Item	Checklist Item	Page
Title and abstract			
Title	1	Identify the study as developing and/or validating a multivariable prediction model, the target population, and the outcome to be predicted.	1
Abstract	2	Provide a summary of objectives, study design, setting, participants, sample size, predictors, outcome, statistical analysis, results, and conclusions.	3
Introduction			
Background and objectives	3a	Explain the medical context (including whether diagnostic or prognostic) and rationale for developing or validating the multivariable prediction model, including references to existing models.	4-5
	3b	Specify the objectives, including whether the study describes the development or validation of the model or both.	4-5
Methods			
Source of data	4a	Describe the study design or source of data (e.g., randomized trial, cohort, or registry data), separately for the development and validation data sets, if applicable.	6
	4b	Specify the key study dates, including start of accrual; end of accrual; and, if applicable, end of follow-up.	5
Participants	5a	Specify key elements of the study setting (e.g., primary care, secondary care, general population) including number and location of centres.	5
	5b	Describe eligibility criteria for participants.	6
	5c	Give details of treatments received, if relevant.	6
Outcome	6a	Clearly define the outcome that is predicted by the prediction model, including how and when assessed.	6
	6b	Report any actions to blind assessment of the outcome to be predicted.	7
Predictors	7a	Clearly define all predictors used in developing or validating the multivariable prediction model, including how and when they were measured.	Supplement
	7b	Report any actions to blind assessment of predictors for the outcome and other predictors.	Supplement
Sample size	8	Explain how the study size was arrived at.	Supplement
Missing data	9	Describe how missing data were handled (e.g., complete-case analysis, single imputation, multiple imputation) with details of any imputation method.	Supplement
Statistical analysis methods	10a	Describe how predictors were handled in the analyses.	Supplement
	10b	Specify type of model, all model-building procedures (including any predictor selection), and method for internal validation.	Supplement
	10d	Specify all measures used to assess model performance and, if relevant, to compare multiple models.	8-9, Supplement
Risk groups	11	Provide details on how risk groups were created, if done.	Not done
Results			
Participants	13a	Describe the flow of participants through the study, including the number of participants with and without the outcome and, if applicable, a summary of the follow-up time. A diagram may be helpful.	9
	13b	Describe the characteristics of the participants (basic demographics, clinical features, available predictors), including the number of participants with missing data for predictors and outcome.	9
Model development	14a	Specify the number of participants and outcome events in each analysis.	9
	14b	If done, report the unadjusted association between each candidate predictor and outcome.	Not done
Model specification	15a	Present the full prediction model to allow predictions for individuals (i.e., all regression coefficients, and model intercept or baseline survival at a given time point).	Feature importa
	15b	Explain how to the use the prediction model.	11-14
Model performance	16	Report performance measures (with CIs) for the prediction model.	10-11
Discussion			
Limitations	18	Discuss any limitations of the study (such as nonrepresentative sample, few events per predictor, missing data).	13-14
Interpretation	19b	Give an overall interpretation of the results, considering objectives, limitations, and results from similar studies, and other relevant evidence.	11-14
Implications	20	Discuss the potential clinical use of the model and implications for future research.	11-14
Other information			
Supplementary information	21	Provide information about the availability of supplementary resources, such as study protocol, Web calculator, and data sets.	Supplement
Funding	22	Give the source of funding and the role of the funders for the present study.	1,14

We recommend using the TRIPOD Checklist in conjunction with the TRIPOD Explanation and Elaboration document.

Supplemental Table 1. TRIPOD Checklist.

Supplemental Table 2. Littenberg framework for the assessment of medical technology as applied to BRAIN A-I

Framework Domain	Description	Applicability to BRAIN A-I
Biologic Plausibility	Does the current understanding of biology and disease pathology support the technology?	Practicing pediatric neurointensive care physicians posit that structured data including laboratory results, vital signs, medications, and other non-laboratory diagnostics can collectively be used to assess a child's risk of incurring or manifesting brain injury during the course of critical illness.
Technical Feasibility	Can the developed technology safely and reliably be delivered to the target patients?	Developing the model in adherance to the United States core data for interoperability and related informatics standard nomenclatures for structured data will facilitate model deployment.
Intermediate Outcomes	What are the biological, physiologic, or clinical effects of the technology?	During this development stage, model-calculated probabilities of neurologic deterioration were assessed for correlation with an available sample of measured, serum-based, brain-derived biomarkers.
Patient Outcomes	Are the intended patient outcomes promoted by use of the technology compatible with overall improved health?	The developed model is intended to alert clinicians but not prescribe a course of action, in large part owing to the complexity and heterogeneity of neurologic morbidity that occurs among critically ill children. Clinicians remain the ultimate arbiters of bedside decision-making that adequately accounts for the balance of risk and benefits related to a given management course.
Societal Outcomes	What are the external effects of the technology and does it confer benefit to the larger society?	Leveraging interoperability standards helps to reduce costs associated with technology deployment. By aiding clinicians in potentially obviating the occurrence or mitigating the effects of neurologic injury multiple population-level benefits are realized, including but not limited to a reduction in societal costs associated with long-term care of profound neurologic injury.

Supplemental Table 3. Data curation steps for individual data elements for the BRAIN AI outcome.

File_Path	Outcome Marker	Type
bh.csv	Behavioral Health Consult	behavioral
haldol.csv	Haloperidol	medication
olanzapine.csv	Olanzapine	medication
dexmedetomidine.csv	Dexmedetomidine	medication
eeg.csv	EEG	neuro
ct.csv	CT Head	neuro
mri.csv	MRI Brain	neuro

Supplemental Table 4. Data curation steps for individual data elements for BRAIN A-I

Data Element	Min	Max	Action	Type	Available at Both Sites
Base deficit	-30	0	Discard	Numerical	Yes
Base excess	0	30	Discard	Numerical	Yes
Bicarbonate	0	80	Discard	Numerical	Yes
Blood urea nitrogen	0	200	Truncate	Numerical	Yes
Chloride	60	190	Discard	Numerical	Yes
Cisatracurium	0	1	Ignore	Boolean	Yes
C-Reactive Protein	0	100	Discard	Numerical	Yes
Creatinine	0.1	25	Discard	Numerical	Yes
CRRT Therapy Type	0	1	Discard	Boolean	No
DBP	0	200	Discard	Numerical	Yes
Dobutamine	0	1	Ignore	Boolean	Yes
Dopamine	0	1	Ignore	Boolean	Yes
ECMO Type	0	1	Discard	Boolean	No
Endotracheal tube	0	1	Discard	Boolean	No
Epinephrine	0	1	Ignore	Boolean	Yes
Fentanyl	0	1	Ignore	Boolean	Yes
Glucose	0	2000	Discard	Numerical	Yes
Hemoglobin	0	30	Discard	Numerical	Yes
Hydromorphone	0	1	Ignore	Boolean	Yes
INR	0	25	Discard	Numerical	No
Lactate	0	30	Discard	Numerical	Yes
Lorazepam	0	1	Ignore	Numerical	Yes
MBP	0	160	Discard	Numerical	Yes
Midazolam	0	1	Ignore	Boolean	Yes
Milrinone	0	1	Ignore	Boolean	Yes
Morphine	0	1	Ignore	Boolean	Yes
Norepinephrine	0	1	Ignore	Boolean	Yes
pCO2	5	150	Discard	Numerical	Yes
Peds Coma Score	3	15	Discard	Numerical	Yes
pH	6	8	Discard	Numerical	Yes
Platelets	0	5000	Discard	Numerical	Yes
Potassium	0.05	12	Discard	Numerical	Yes
Procalcitonin	0	250	Discard	Numerical	Yes
PTT	0	250	Truncate	Numerical	Yes
Pulse	0	350	Discard	Numerical	Yes
Pupillary Reaction				Categorical	Yes
Respiratory Rate	0	150	Discard	Numerical	Yes
SBP	0	300	Discard	Numerical	Yes
Sodium	80	215	Discard	Numerical	Yes
SpO2	0	100	Discard	Numerical	Yes
Temperature	0	46	Discard	Numerical	Yes

Ventilated	0	1	Discard	Boolean	Yes
Ventilator Make/Model				Categorical	Yes
Weight	0	300	Discard	Numerical	Yes
White blood cell count	0	300	Discard	Numerical	Yes

Supplemental Table 5. Standard vocabulary crosswalk for BRAIN-AI components

BRAIN A-I Components	Cerner Millennium Code Set	Standard Vocabulary	Standard Identifier	Standard Display	USCDI
Laboratory Tests					
Base deficit	72 (Clinical Event Observation)	LOINC	1922-4	Base deficit in Arterial blood	Version 1
			1923-2	Base deficit in Capillary blood	
			1924-0	Base deficit in Venous blood	
			30318-0	Base deficit in Blood	
Base excess	72 (Clinical Event Observation)	LOINC	11555-0	Base excess in Blood by calculation	Version 1
			1925-7	Base excess in Arterial blood by calculation	
			1926-5	Base excess in Capillary blood by calculation	
			1927-3	Base excess in Venous blood by calculation	
Bicarbonate	72 (Clinical Event Observation)	LOINC	1959-6	Bicarbonate [Moles/volume] in Blood	Version 1
			1960-4	Bicarbonate [Moles/volume] in Arterial blood	
			1961-2	Bicarbonate [Moles/volume] in Capillary blood	
			14627-4	Bicarbonate [Moles/volume] in Venous blood	
			2028-9	Carbon dioxide, total [Moles/volume] in Serum or Plasma	
			20565-8	Carbon dioxide, total [Moles/volume] in Blood	
Blood urea nitrogen	72 (Clinical Event Observation)	LOINC	3094-0	Urea nitrogen [Mass/volume] in Serum or Plasma	Version 1
			6299-2	Urea nitrogen [Mass/volume] in Blood	
Chloride	72 (Clinical Event Observation)	LOINC	2075-0	Chloride [Moles/volume] in Serum or Plasma	Version 1
			2069-3	Chloride [Moles/volume] in Blood	
C-reactive protein	72 (Clinical Event Observation)	LOINC	1988-5	C reactive protein [Mass/volume] in Serum or Plasma	Version 1
Creatinine	72 (Clinical Event Observation)	LOINC	2160-0	Creatinine [Mass/volume] in Serum or Plasma	Version 1
			38483-4	Creatinine [Mass/volume] in Blood	
Glucose	72 (Clinical Event Observation)	LOINC	41653-7	Glucose [Mass/volume] in Capillary blood by Glucometer	Version 1
			2345-7	Glucose [Mass/volume] in Serum or Plasma	
			2339-0	Glucose [Mass/volume] in Blood	
Hemoglobin	72 (Clinical Event Observation)	LOINC	718-7	Hemoglobin [Mass/volume] in Blood	Version 1
			30351-1	Hemoglobin [Mass/volume] in Mixed venous blood	
			30313-1	Hemoglobin [Mass/volume] in Arterial blood	
			30350-3	Hemoglobin [Mass/volume] in Venous blood	
International normalized ratio	72 (Clinical Event Observation)	LOINC	6301-6	INR in Platelet poor plasma by Coagulation assay	Version 1
Lactate	72 (Clinical Event Observation)	LOINC	2519-7	Lactate [Moles/volume] in Venous blood	Version 1
			32693-4	Lactate [Moles/volume] in Blood	
Partial pressure of carbon dioxide	72 (Clinical Event Observation)	LOINC	2020-6	Carbon dioxide [Partial pressure] in Capillary blood	Version 1
			11557-6	Carbon dioxide [Partial pressure] in Blood	
			2019-8	Carbon dioxide [Partial pressure] in Arterial blood	
pH	72 (Clinical Event Observation)	LOINC	2745-8	pH of Capillary blood	Version 1
			11558-4	pH of Blood	
			2744-1	pH of Arterial blood	
			2746-6	pH of Venous blood	
Platelets	72 (Clinical Event Observation)	LOINC	777-3	Platelets [#/volume] in Blood by Automated count	Version 1

Supplemental Table 5. Standard vocabulary crosswalk for BRAIN-AI components

BRAIN A-I Components	Cerner Millennium Code Set	Standard Vocabulary	Standard Identifier	Standard Display	USCDI
Potassium	72 (Clinical Event Observation)	LOINC	2823-3	Potassium [Moles/volume] in Serum or Plasma	Version 1
			6298-4	Potassium [Moles/volume] in Blood	
Procalcitonin	72 (Clinical Event Observation)	LOINC	33959-8	Procalcitonin [Mass/volume] in Serum or Plasma	Version 1
Partial thromboplastin time	72 (Clinical Event Observation)	LOINC	14979-9	aPTT in Platelet poor plasma by Coagulation assay	Version 1
Sodium	72 (Clinical Event Observation)	LOINC	2951-2	Sodium [Moles/volume] in Serum or Plasma	Version 1
			2947-0	Sodium [Moles/volume] in Blood	
White blood cell count	72 (Clinical Event Observation)	LOINC	6690-2	Leukocytes [#/volume] in Blood by Automated count	Version 1
			49498-9	Leukocytes [#/volume] in Blood by Estimate	
Vital signs					
Diastolic blood pressure	72 (Clinical Event Observation)	LOINC	8453-3	Diastolic blood pressure--sitting	Version 1
			8454-1	Diastolic blood pressure--standing	
			8455-8	Diastolic blood pressure--supine	
			8462-4	Diastolic blood pressure	
Glasgow coma scale score	72 (Clinical Event Observation)	LOINC	9269-2	Glasgow coma score total	Version 3
			9270-0	Glasgow coma score verbal	
			9267-6	Glasgow coma score eye opening	
			9268-4	Glasgow coma score motor	
Heart rate	72 (Clinical Event Observation)	LOINC	68999-2	Heart rate --supine	Version 1
			69000-8	Heart rate --sitting	
			69001-6	Heart rate --standing	
			8867-4	Heart rate	
			8890-6	Heart rate Cardiac apex by Auscultation	
Mean blood pressure	72 (Clinical Event Observation)	LOINC	8478-0	Mean blood pressure	Version 1
Pulse oximetry	72 (Clinical Event Observation)	LOINC	59408-5	Oxygen saturation in Arterial blood by Pulse oximetry	Version 1
Respiratory rate	72 (Clinical Event Observation)	LOINC	9279-1	Respiratory rate	Version 1
Systolic blood pressure	72 (Clinical Event Observation)	LOINC	8480-6	Systolic blood pressure	Version 1
Temperature	72 (Clinical Event Observation)	LOINC	60836-4	Esophageal temperature	Version 1
			76278-1	Bladder temperature via Foley	
			8310-5	Body temperature	
			8328-7	Axillary temperature	
			8329-5	Body temperature - Core	
			8331-1	Oral temperature	
			8332-9	Rectal temperature	
			8334-5	Body temperature – Urinary bladder	
Ventilator interface	72 (Clinical Event Observation)	LOINC	LL5542-7	Intubation tube types	Medical Device Class - Version Unknown
Ventilator make	72 (Clinical Event Observation)	LOINC	LL7706-7	Ventilator	Medical Device Class - Version Unknown
Weight	72 (Clinical Event Observation)	LOINC	29463-7	Body weight	Version 1
Medications					
Cisatracurium (Intravenous)	72 (Clinical Event Observation)	RxNorm RXCUI	319864	cisatracurium	Version 1
Dexmedetomidine (Intravenous)	72 (Clinical Event Observation)	RxNorm RXCUI	48937	dexmedeTOMIDine	Version 1

Supplemental Table 5. Standard vocabulary crosswalk for BRAIN-AI components

BRAIN A-I Components	Cerner Millennium Code Set	Standard Vocabulary	Standard Identifier	Standard Display	USCDI
Dobutamine (Intravenous)	72 (Clinical Event Observation)	RxNorm RXCUI	3616	DOBUTamine	Version 1
Dopamine (Intravenous)	72 (Clinical Event Observation)	RxNorm RXCUI	3628	dopamine	Version 1
Epinephrine (Intravenous)	72 (Clinical Event Observation)	RxNorm RXCUI	3992	EPINEPHrine	Version 1
Fentanyl (Intravenous)	72 (Clinical Event Observation)	RxNorm RXCUI	4337	fentaNYL	Version 1
Haldol	72 (Clinical Event Observation)	RxNorm RXCUI	151839	Haldol	Version 1
Hydromorphone (Intravenous)	72 (Clinical Event Observation)	RxNorm RXCUI	3423	HYDROmorphone	Version 1
Lorazepam (Intravenous)	72 (Clinical Event Observation)	RxNorm RXCUI	6470	LORazepam	Version 1
Midazolam (Intravenous)	72 (Clinical Event Observation)	RxNorm RXCUI	6960	midazolam	Version 1
Milrinone (Intravenous)	72 (Clinical Event Observation)	RxNorm RXCUI	52769	milrinone	Version 1
Morphine (Intravenous)	72 (Clinical Event Observation)	RxNorm RXCUI	7052	morphine	Version 1
Norepinephrine (Intravenous)	72 (Clinical Event Observation)	RxNorm RXCUI	7512	norepinephrine	Version 1
Olanzapine	72 (Clinical Event Observation)	RxNorm RXCUI	61381	OLANZapine	Version 1
Non-Laboratory Diagnostics					
Brain computed tomography	72 (Clinical Event Observation)	LOINC	24725-4	CT Head	Version 2
Brain magnetic resonance imaging	72 (Clinical Event Observation)	LOINC	24590-2	MR Brain	Version 2
Electroencephalogram	72 (Clinical Event Observation)	LOINC	11523-8	EEG study	Version 2
Pupillary reaction	72 (Clinical Event Observation)	LOINC	79899-1	Left pupil Pupillary response	Observation Class – Version Unknown
		LOINC	79815-7	Right pupil Pupillary response	Observation Class – Version Unknown
Consultation					
Behavioral health consult	72 (Clinical Event Observation)	SNOMED CT	733870009	Assessment of delirium	Observation Class – Version Unknown

Abbreviations: aPTT, activated partial thromboplastin time; BRAIN A-I, biodigital rapid alert for identifying neuromorbidity A-I bundle; CT, computed tomography; EEG, electroencephalography; MR, magnetic resonance; LOINC, logical object identifiers, names, and codes; RXCUI, RxNorm concept unique identifier; SNOMED CT, systematized nomenclature of medicine - clinical terms; USCDI, United States Core Data for Interoperability

Supplemental Table 6. Predictive performance of the XGBoost model with a 12-hour censor horizon and 48-hour feature window in the validation dataset, after manual tuning, and after Bayesian tuning.

	XGBoost Base	XGBoost Manual Tuning	XGBoost Bayesian Tuning
AUROC	0.84	0.84	0.85
AUPRC	0.61	0.62	0.63
F1 Score	0.54	0.56	0.58
PPV	0.77	0.75	0.63
NPV	0.92	0.92	0.93
Sensitivity	0.41	0.44	0.54
Specificity	0.98	0.98	0.95

Models were tuned to optimize the F1 score, bordered in bold.
Abbreviations: AUPRC, area under the precision recall curve; AUROC, area under the receiver operating characteristics curve; NPV, negative predictive value; PPV, positive predictive value; XGBoost, extreme gradient boosting.

Supplemental Table 7. Predictive performance of the XGBoost model with a 12-hour censor horizon and 48-hour feature window in the test dataset, after manual tuning, and after Bayesian tuning.

	XGBoost Base	XGBoost Manual Tuning	XGBoost Bayesian Tuning
AUROC	0.87	0.88	0.89
AUPRC	0.66	0.68	0.69
F1 Score	0.57	0.58	0.62
PPV	0.86	0.79	0.74
NPV	0.93	0.93	0.94
Sensitivity	0.43	0.46	0.53
Specificity	0.99	0.98	0.98

Models were tuned to optimize the F1 score, bordered in bold.
Abbreviations: AUPRC, area under the precision recall curve; AUROC, area under the receiver operating characteristics curve; NPV, negative predictive value; PPV, positive predictive value; XGBoost, extreme gradient boosting.

Supplemental Table 8. Cohort ascertainment and exclusions for varied censored time horizons and feature windows at the development site.

Encounters with a PICU admission	**32,702**								
Feature window (hours)	24			48			72		
Censored time Horizon (hours)	6	12	24	6	12	24	6	12	24
Visit length or time to outcome hours less than feature window + time horizon	2925	3435	3908	7720	8230	8703	11593	12103	12576
Outcome occurred before PICU admission	4956								
Missing age, admission time, or discharge time	821								
PICU length of stay <1 hour	182								
No documented SpO_2 measurement	7								
Discharge time documented prior to admission time	2								
Final cohort	**23873**	**23363**	**22890**	**19078**	**18568**	**18095**	**15205**	**14695**	**14222**
Cases	**2841**	**2331**	**1858**	**2841**	**2331**	**1858**	**2841**	**2331**	**1858**
Controls	**21032**			**16237**			**12364**		

Cohort numbers in **bold** represent the cohort at a given stage of ascertainment and numbers not in bold represent encounter dropout at stages of cleaning.

Supplemental Table 9. Performance of the optimal models in the validation dataset at the development site.

	Development Site								
Feature Window (hours)	**24**			**48**			**72**		
Censored Time Horizon (hours)	**6**	**12**	**24**	**6**	**12**	**24**	**6**	**12**	**24**
Model	LR	LR	LR	XGB	XGB	LR	XGB	LR	XGB
Feature Selection	IG	IG	IG	IG	IG	IG	IG	IG	IG
AUROC	0.83	0.83	0.80	0.87	0.82	0.82	0.88	0.86	0.82
AUPRC	0.59	0.49	0.39	0.73	0.61	0.53	0.78	0.71	0.61
PPV	0.74	0.65	0.60	0.82	0.79	0.69	0.88	0.75	0.68
NPV	0.92	0.92	0.93	0.92	0.92	0.93	0.91	0.92	0.92
Sensitivity	0.40	0.29	0.24	0.53	0.41	0.41	0.58	0.54	0.47
Specificity	0.98	0.98	0.99	0.98	0.98	0.98	0.98	0.97	0.97

Abbreviations: AUROC, area under the receiver operating characteristics curve; AUPRC, area under the precision recall curve; CFS, correlation-based feature selection; IG, information gain; LR, logistic regression; NB, naïve Bayes; NPV, negative predictive value; PPV, positive predictive value; XGB, XGBoost (extreme gradient boosting)

Supplemental Table 10. F1 scores of top performing models in the development site validation dataset.

		Censored Time Horizon		
		6-hours	**12-hours**	**24-hours**
Feature Window	**24-hours**	LR 0.52	LR 0.40	LR 0.34
	48-hours	XGB 0.65	XGB 0.54	LR 0.51
	72-hours	XGB 0.70	LR 0.65	XGB 0.57

Cells denote the best performing model and the F1 score / Brier score.
All models at the development site were created using information gain feature selection
Abbreviations: LR, logistic regression; XGB, XGBoost (extreme gradient boosting)

Supplemental Table 11A. F_β (β=2) scores of top performing models in the development site validation dataset.

		Censored Time Horizon		
		6-hours	**12-hours**	**24-hours**
Feature Window	**24-hours**	XGB 0.44 (0.44)	XGB 0.33 (0.32)	LR 0.27 (0.25)
	48-hours	LR 0.59 (0.58)	LR 0.49 (0.45)	LR 0.45 (0.39)
	72-hours	LR 0.66 (0.61)	LR 0.58 (0.55)	LR 0.51 (0.46)

Cells denote the best performing model and the F_β (β=2) score. XGB and LR were the top performing models. Values within each bracket are the F_β (β=2) scores of the other model.
All models at the development site were created using information gain feature selection.
Abbreviations: LR, logistic regression; XGB, XGBoost (extreme gradient boosting)

Supplemental Table 11B. F_β (β=3) scores of top performing models in the development site validation dataset.

		Censored Time Horizon		
		6-hours	**12-hours**	**24-hours**
Feature Window	**24-hours**	XGB 0.42 (0.42)	XGB 0.31 (0.30)	LR 0.26 (0.24)
	48-hours	LR 0.58 (0.55)	LR 0.48 (0.43)	LR 0.43 (0.37)
	72-hours	LR 0.64 (0.59)	LR 0.56 (0.53)	LR 0.50 (0.44)

Cells denote the best performing model and the F_β (β=3) score. XGB and LR were the top performing models. Values within each bracket are the F_β (β=3) scores of the other model. All models at the development site were created using information gain feature selection.
Abbreviations: LR, logistic regression; XGB, XGBoost (extreme gradient boosting)

Supplemental Table 11C. F_β (β=0.5) scores of top performing models in the development site validation dataset.

		Censored Time Horizon		
		6-hours	**12-hours**	**24-hours**
Feature Window	**24-hours**	XGB 0.62 (0.62)	XGB 0.52 (0.51)	LR 0.46 (0.46)
	48-hours	XGB 0.76 (0.72)	XGB 0.65 (0.64)	LR 0.61 (0.60)
	72-hours	XGB 0.79 (0.77)	XGB 0.73 (0.70)	XGB 0.67 (0.64)

Cells denote the best performing model and the F_β (β=0.5) score. XGB and LR were the top performing models. Values within each bracket are the F_β (β=0.5) scores of the other model.
All models at the development site were created using information gain feature selection.
Abbreviations: LR, logistic regression; XGB, XGBoost (extreme gradient boosting)

Supplemental Table 12A. Statistical performance of the 12-hour time horizon, 48-hour feature window XGBoost and logistic regression models over a range of score thresholds in the development site validation dataset.

Threshold	AUROC	AUPRC	F1 Score	F2 Score	F3 Score	F0.5 Score	PPV	NPV	Sensitivity	Specificity	Confusion Matrix - (TN, FP, FN,TP)
XGBoost Model											
0.025			0.361	0.542	**0.650**	0.271	0.232	**0.956**	**0.813**	0.602	(1879, 1242, 86, 375)
0.05			0.422	**0.554**	0.619	0.341	0.302	0.945	0.701	0.761	(2375, 746, 138, 323)
0.1			0.483	**0.554**	0.582	0.429	0.399	0.938	0.614	0.863	(2694, 427, 178, 283)
0.3	0.818	0.601	**0.553**	0.508	0.494	0.607	0.649	0.926	0.482	0.962	(3001, 120, 239, 222)
0.5			0.536	0.454	0.432	0.654	0.766	0.919	0.412	0.981	(3063, 58, 271, 190)
0.7			0.508	0.411	0.386	**0.664**	0.836	0.913	0.364	0.989	(3088, 33, 293, 168)
0.9			0.429	0.325	0.301	0.629	**0.915**	0.904	0.280	**0.996**	(3109, 12, 332, 129)
Logistic Regression Model											
0.025			0.318	0.518	0.656	0.229	0.193	**0.966**	**0.894**	0.449	(1402, 1719, 49, 412)
0.05			0.384	0.561	**0.662**	0.292	0.252	0.958	0.809	0.645	(2012, 1109, 88, 373)
0.1			0.452	**0.574**	0.631	0.372	0.333	0.947	0.701	0.793	(2475, 646, 138, 323)
0.3	0.827	0.610	0.549	0.538	0.535	0.561	0.568	0.931	0.531	0.940	(2935, 186, 216, 245)
0.5			**0.557**	0.494	0.477	0.638	0.707	0.924	0.460	0.972	(3033, 88, 249, 212)
0.7			0.533	0.444	0.420	**0.668**	0.803	0.917	0.399	0.986	(3076, 45, 277, 184)
0.9			0.450	0.346	0.321	0.645	**0.908**	0.906	0.299	**0.996**	(3107, 14, 323, 138)

Supplemental Table 12B. Statistical performance of the 12-hour time horizon, 48-hour feature window XGBoost model over a range of score thresholds in the development site test dataset.

Threshold	AUROC	AUPRC	F1 Score	F2 Score	F3 Score	F0.5 Score	PPV	NPV	Sensitivity	Specificity	Confusion Matrix - (TN, FP, FN,TP)
XGBoost Model											
0.025			0.399	0.587	**0.698**	0.302	0.260	**0.974**	**0.859**	0.682	(2559, 1195, 69, 419)
0.05			0.493	0.621	0.679	0.409	0.367	0.962	0.750	0.832	(3124, 630, 122, 366)
0.1			0.573	**0.623**	0.642	0.531	0.505	0.954	0.662	0.916	(3438, 316, 165, 323)
0.3	0.873	0.671	**0.603**	0.538	0.519	0.685	0.754	0.938	0.502	0.979	(3674, 80, 243, 245)
0.5			0.562	0.463	0.437	**0.715**	0.874	0.929	0.414	0.992	(3725, 29, 286, 202)
0.7			0.491	0.383	0.357	0.684	0.926	0.920	0.334	0.997	(3741, 13, 325, 163)
0.9			0.390	0.287	0.264	0.610	**0.975**	0.910	0.244	**0.999**	(3751, 3, 369, 119)

Supplemental Table 13. Cohort ascertainment and exclusions for varied feature windows for the validation site.	
Timeframe	**4/2018-2023**
Encounters with a PICU admission	**9,039**
Feature Window	48-hours
Visit length <24 hours or PICU length of stay <1 hour	1,791
Missing age, discharge time or sex	329
No documented SpO_2 measurement	15
No accurate Neuro Consultation records prior 2018	---
Outcome event prior to PICU admission	79
Key data missing within Feature Window	---
Final Cohort	**6,825**
Cases	**387**
Controls	**6,438**

Supplemental Table 14. Statistical performance of the extreme gradient boosting (XGBoost) and logistic regression generalizable models at the development site across varied output thresholds.

Threshold	AUROC	AUPRC	F1 Score	F2 Score	F3 Score	F0.5 Score	PPV	NPV	Sensitivity	Specificity	Confusion Matrix - (TN, FP, FN,TP)
XGBoost Model											
0.025	0.872	0.617	0.365	0.551	0.665	0.272	0.233	0.976	0.837	0.708	(2658, 1096, 65, 333)
0.05			0.459	0.598	0.666	0.372	0.330	0.970	0.751	0.838	(3147, 607, 99, 299)
0.1			0.528	0.591	0.615	0.478	0.450	0.960	0.641	0.917	(3442, 312, 143, 255)
0.3			0.547	0.481	0.462	0.635	0.711	0.943	0.445	0.981	(3682, 72, 221, 177)
0.5			0.489	0.394	0.370	0.645	0.818	0.935	0.349	0.992	(3723, 31, 259, 139)
0.7			0.421	0.316	0.292	0.629	0.939	0.928	0.271	0.998	(3747, 7, 290, 108)
0.9			0.312	0.222	0.202	0.527	0.974	0.921	0.186	0.999	(3752, 2, 324, 74)
Logistic Regression Model											
0.025	0.855	0.605	0.303	0.497	0.633	0.218	0.183	0.977	0.869	0.590	(2213, 1541, 52, 346)
0.05			0.388	0.552	0.643	0.299	0.260	0.969	0.769	0.767	(2881, 873, 92, 306)
0.1			0.481	0.571	0.609	0.415	0.380	0.960	0.653	0.887	(3330, 424, 138, 260)
0.3			0.562	0.513	0.499	0.621	0.668	0.947	0.485	0.974	(3658, 96, 205, 193)
0.5			0.520	0.429	0.406	0.658	0.801	0.938	0.384	0.990	(3716, 38, 245, 153)
0.7			0.489	0.383	0.357	0.677	0.911	0.934	0.334	0.997	(3741, 13, 265, 133)
0.9			0.367	0.267	0.245	0.584	0.968	0.924	0.226	0.999	(3751, 3, 308, 90)

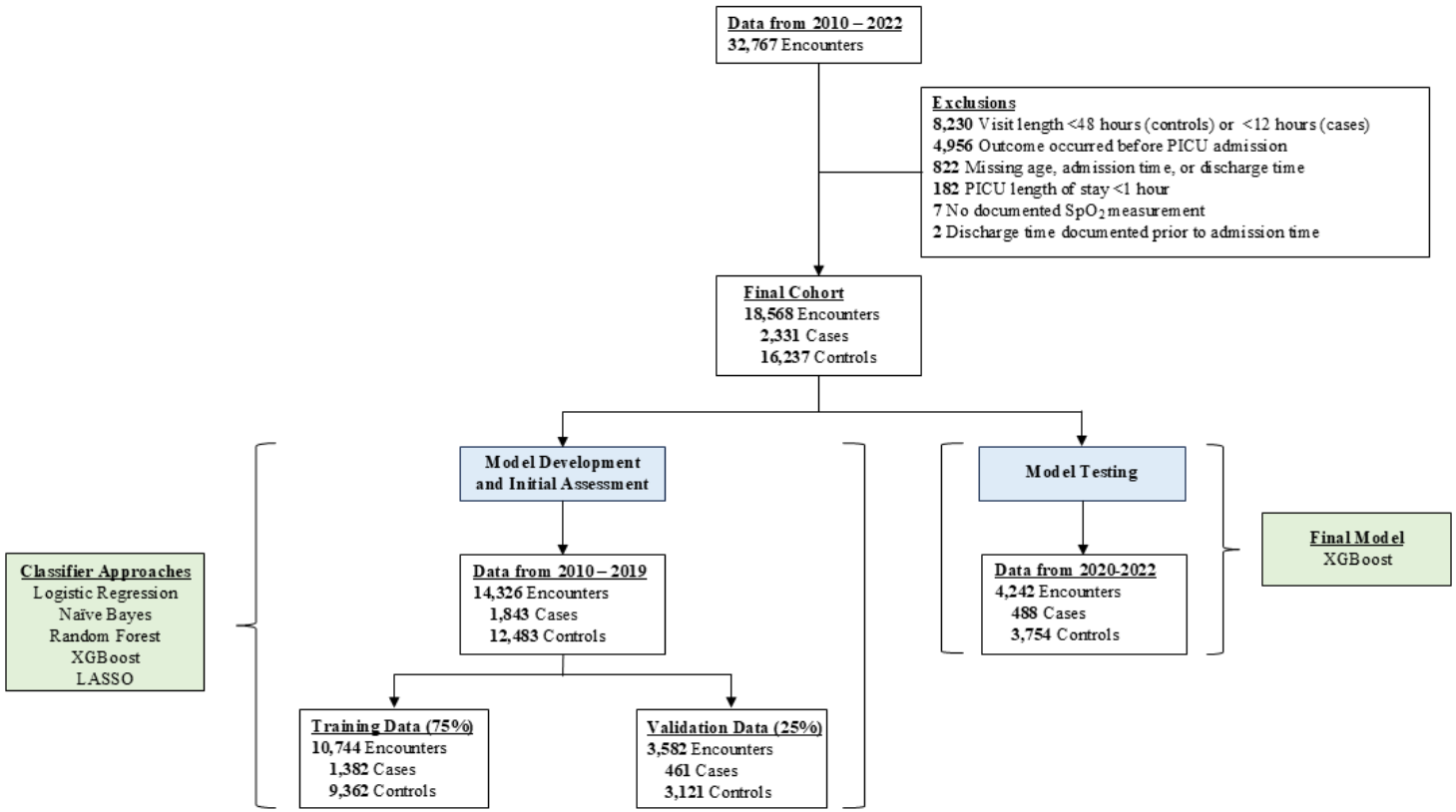

Figure 1. Cohort ascertainment for the final model at the development site, which included features engineered using 48 hours of preceding data and censoring 12-hours prior to the event for cases. Initial model development and validation proceeded using data from 2010-2019. The model was tested using data from 2020-2022. Abbreviations: LASSO, least absolute shrinkage and selection operator; PICU, pediatric intensive care unit; XGBoost, extreme gradient boosting.

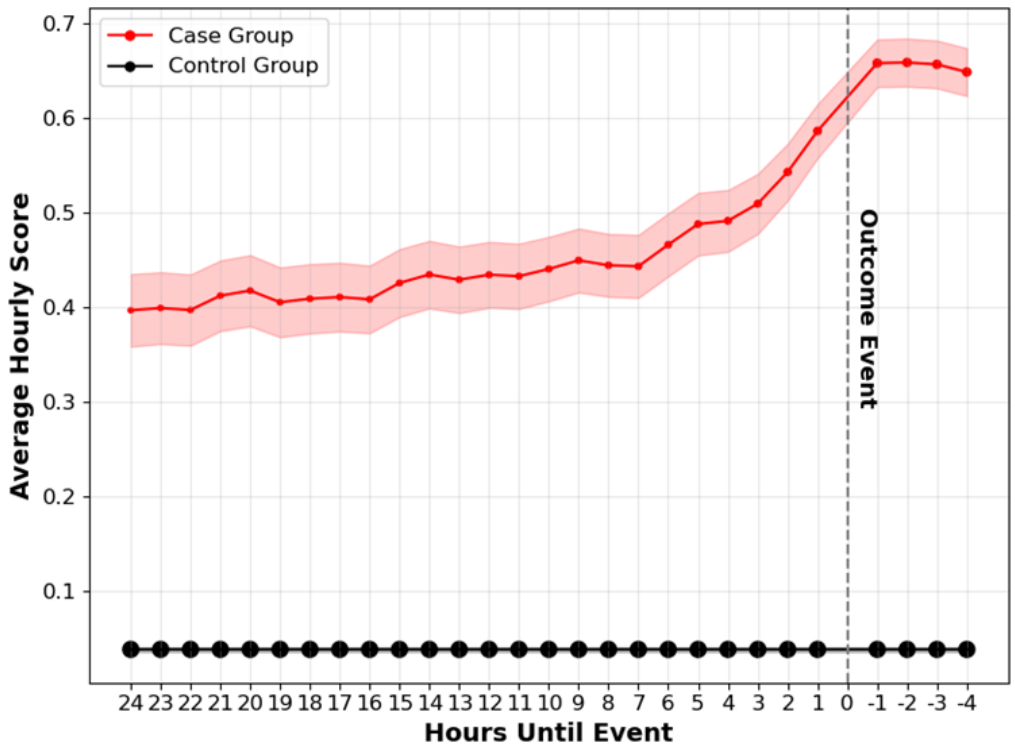

Figure 2. Average hourly scores in the test dataset (encounters with a PICU stay in the year 2020 – 2022) for varied censored time horizon windows for the extreme gradient boosted model developed using a 12-hour time horizon and 48-hour feature window at the development site. The red dots are the average hourly scores 24 hours prior to an event and 4 hours after an event for the case encounters (encounters with an identified neurologic morbidity) and the shaded red region represents the 95% confidence interval. The black dots are the average hourly scores for the control encounters (encounters without an identified neurological morbidity). Confidence intervals for the control encounters are not discernable in the figure due to the large cohort size. The size of the dots is proportionate to the cohort size at that timepoint.

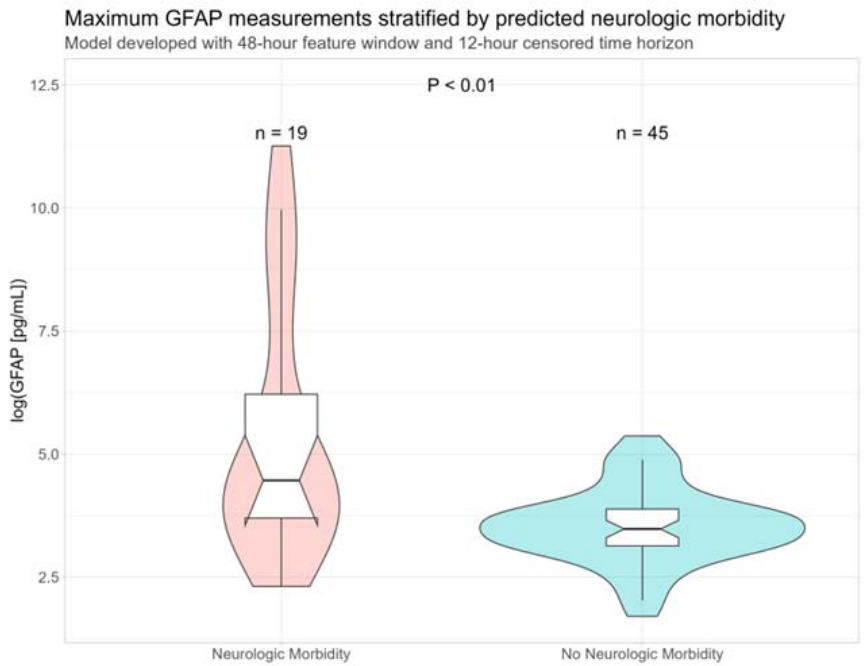

Figure 3. Log-transformed maximum GFAP measurements for a convenience cohort of 64 patients, stratified by predicted neurologic morbidity using the 12-hour time horizon 48-hour feature window extreme gradient boosting model. Abbreviations: GFAP, glial fibrillary acidic protein; mL, milliliter; pg, picogram.

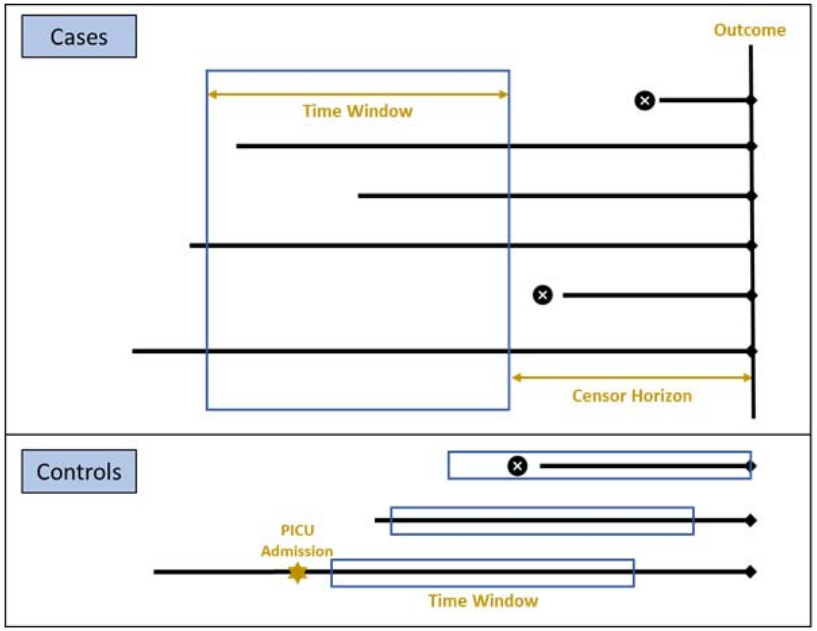

Supplemental Figure 1. A representation of the time window and censor horizons used to define cases and controls as part of the development, validation, and test cohorts. The blue boxes in the top, 'Cases' box identify a time window that is also demarcated by a horizontal, gold, bidirectional arrow, the horizontal black lines represent length of stay for individual encounters, the vertical black line represents the occurrence of the neurological morbidity outcome, and the gold, horizontal, bidirectional arrow indicates the censor horizon, or period of time that data were not incorporated into the model. In the bottom, 'Controls' box, the blue boxes indicate the time window of data used for each stage of model development and evaluation. The white 'x's' in black circles indicate the start of an encounter.

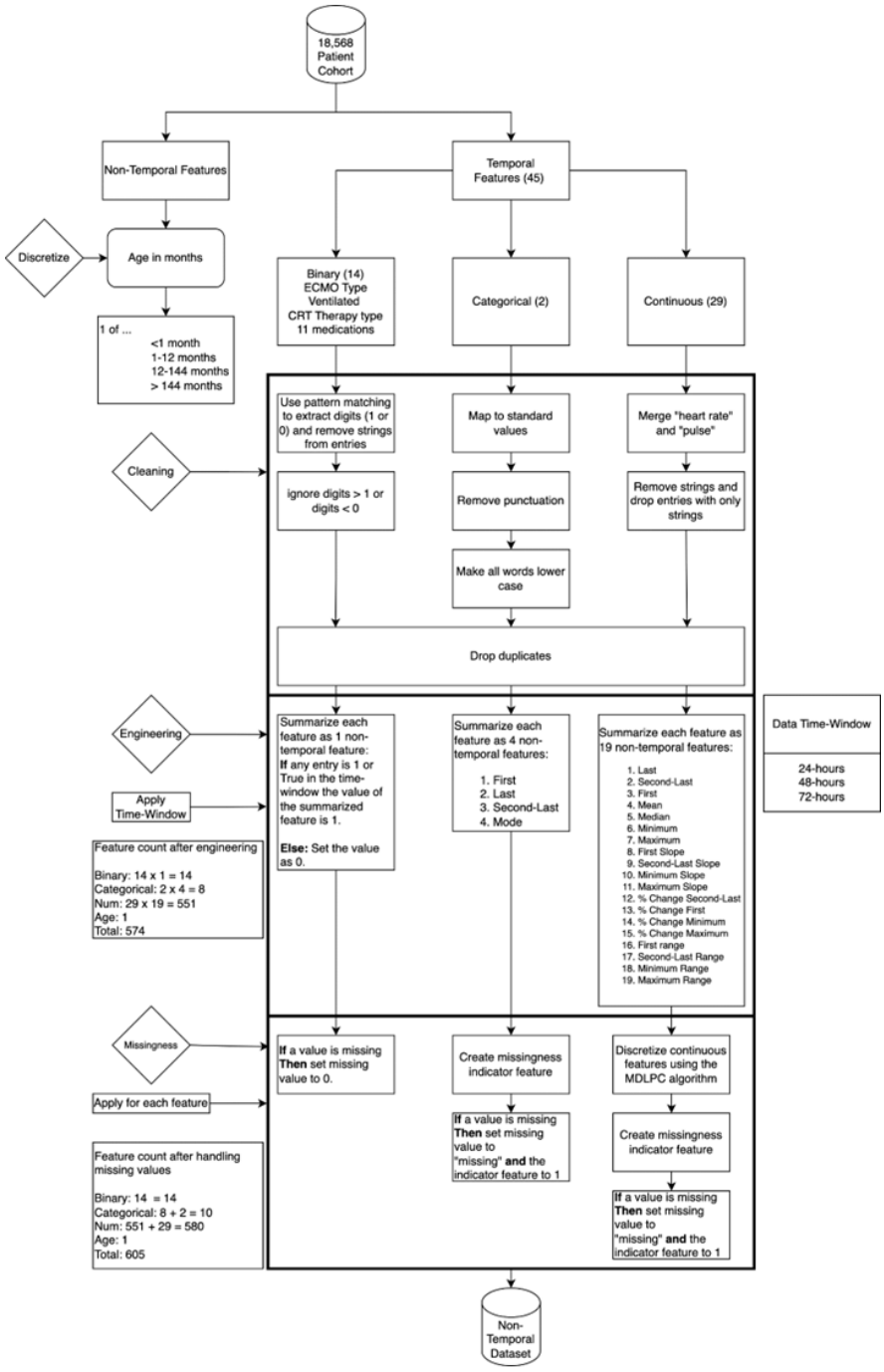

Supplemental Figure 2. Data cleaning and feature engineering process.

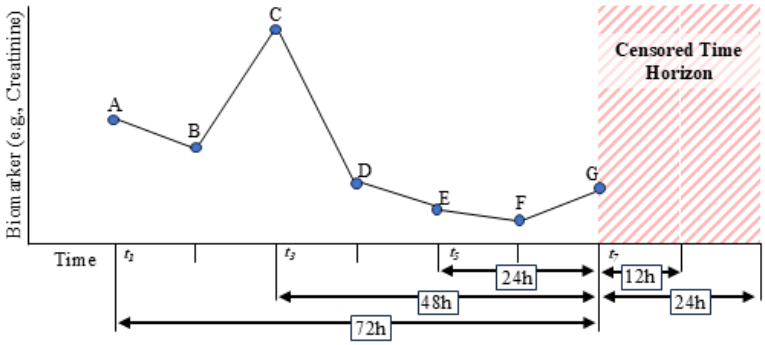

#	Feature	Definition	Example with 24 hours of data
1	Last	The last value prior to the censor window	G
2	Second to last	Second to last value prior to the censor window	F
3	First	First value prior to the censor window	E
4	Mean	Average of the values	(E + F + G) / 3
5	Median	Median of the values	E
6	Minimum	Minimum of the values	F
7	Maximum	Maximum of the values	G
8	First slope	The first measured slope	$(F - E) / (t_6 - t_5)$
9	Second to last slope	Second to last measured slope	$(F - E) / (t_6 - t_5)$
10	Minimum slope	Minimum measured slope	$(F - E) / (t_6 - t_5)$
11	Maximum slope	Maximum measured slope	$(G - F) / (t_7 - t_6)$
12	% change second to last	% difference between the last and second to last value	((G – F) / F) x 100
13	% change first	% difference between the last and first values	((G – E) / E) x 100
14	% change minimum	% difference between the last and minimum values	((G – F) / F) x 100
15	% change maximum	% difference between the last and maximum values	((G – G) / G) x 100
16	First range	Difference between last and first values	G – E
17	Second to last range	Difference between the last and second to last value	G – F
18	Minimum range	Difference between the last and minimum values	G – F
19	Maximum range	Difference between the last and maximum values	G – G

Supplemental Figure 3. A representation of the feature engineering for continuous biomarker measurements. Temporal information is represented as a variety of summary measurements for discrete windows of time. Feature windows of 24-hours, 48-hours, and 72-hours are displayed in the figure. The models at the development site were trained with 6-hour, 12-hour, and 24-hour censored time horizons, with 12-hour and 24-hour horizons demonstrated in the figure. Definitions and related examples for a 24-hour window of data prior to the censor period are displayed in the table. Abbreviations: h, hours.

Adapted from Hauskrecht M, Batal I, Valko M, Visweswaran S, Cooper GF, Clermont G. Outlier detection for patient monitoring and alerting. J Biomed Inform. 2013 Feb;46(1):47-55.

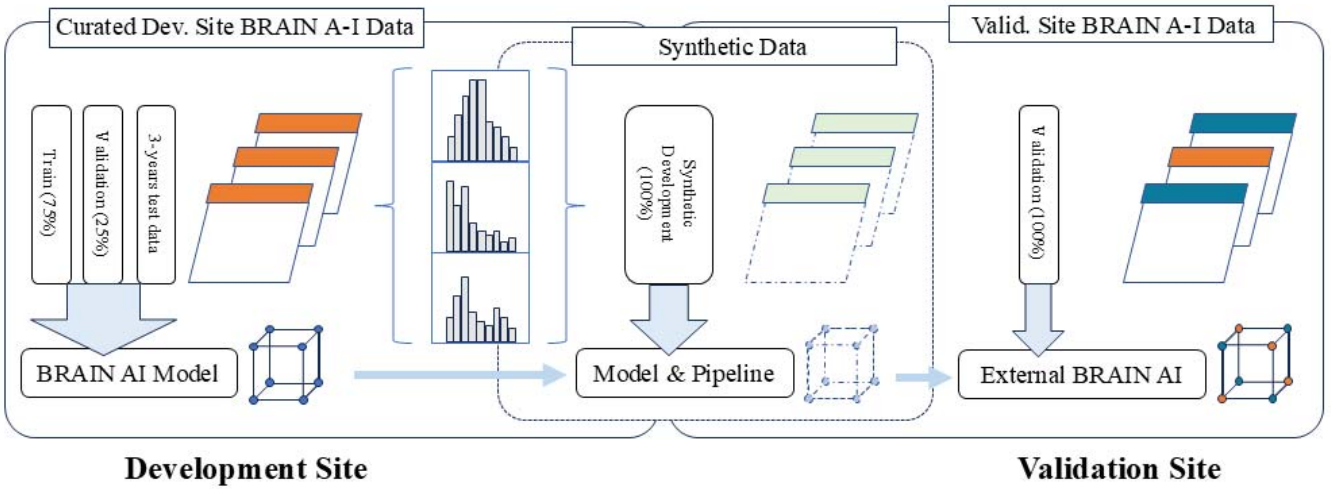

Supplemental Figure 4. The process of BRAIN A-I model development and external validation. Curated data at the development site were divided into a train cohort, validation cohort, and 2-years of holdout test data. The curated data were used to generate synthetic data with comparable single variable statistical distributions. The synthetic data were then distributed to the external validation site with the generalizable model, facilitating local data curation by providing the necessary details of data structure. Finally, the working BRAIN A-I model and pipeline were applied to real-world data at the external validation site. Abbreviations: BRAIN A-I, Biodigital Rapid Alert to Identify Neuromorbidity A-I Bundle; Dev. Site, Development Site; Valid. Site, Validation Site.

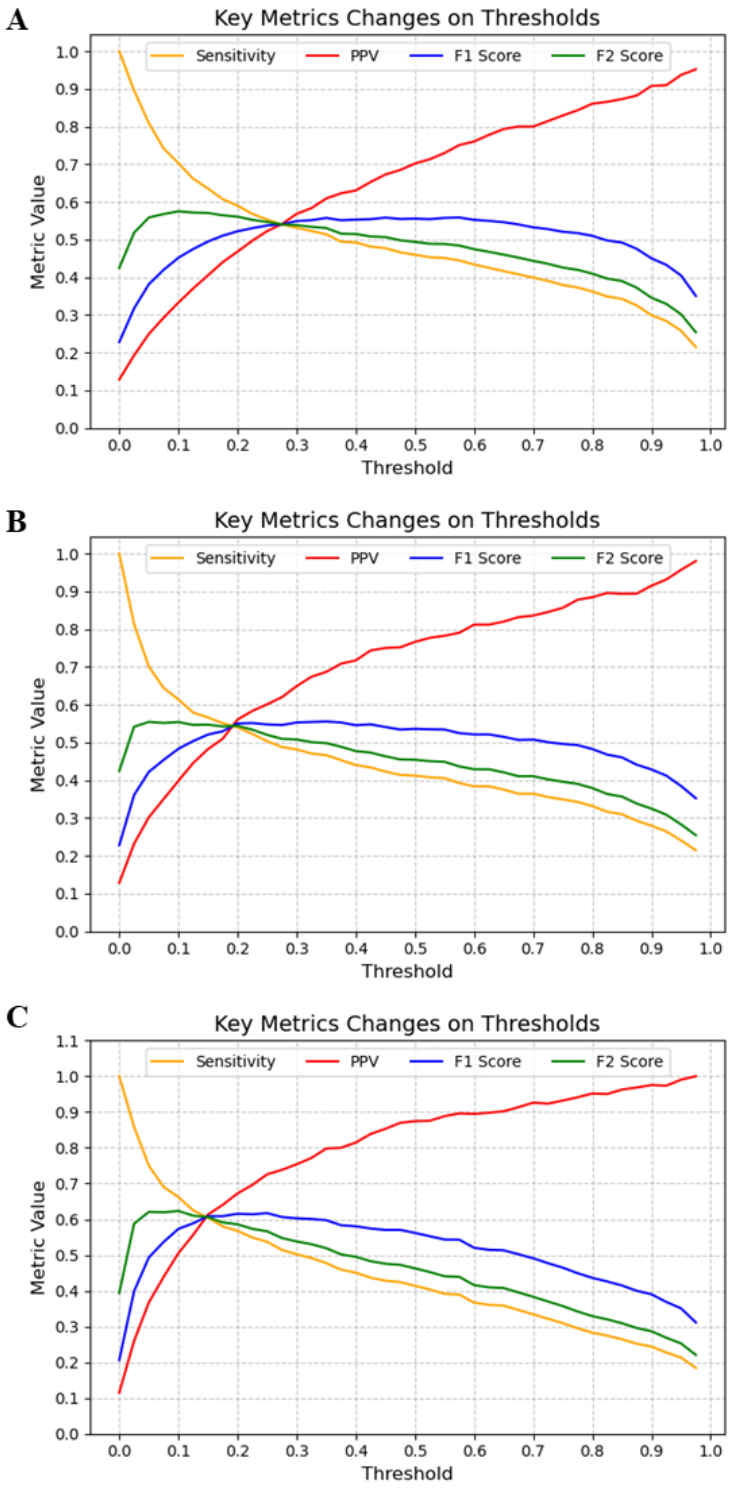

Supplemental Figure 5. Plots the key statistical performance metrics sensitivity (gold line), positive predictive value (PPV, red line), F1 score (blue line), and F2 score (green line) with metric values on the y-axis and model output thresholds on the x-axis for A) the logistic regression model with a 12-hour time horizon and 48-hour feature window in the development site validation dataset; B) the extreme gradient boosting model with a 12-hour time horizon and 48-hour feature window in the development site validation dataset; and C) the extreme gradient boosting model with a 12-hour time horizon and 48-hour feature window in the development site test dataset.

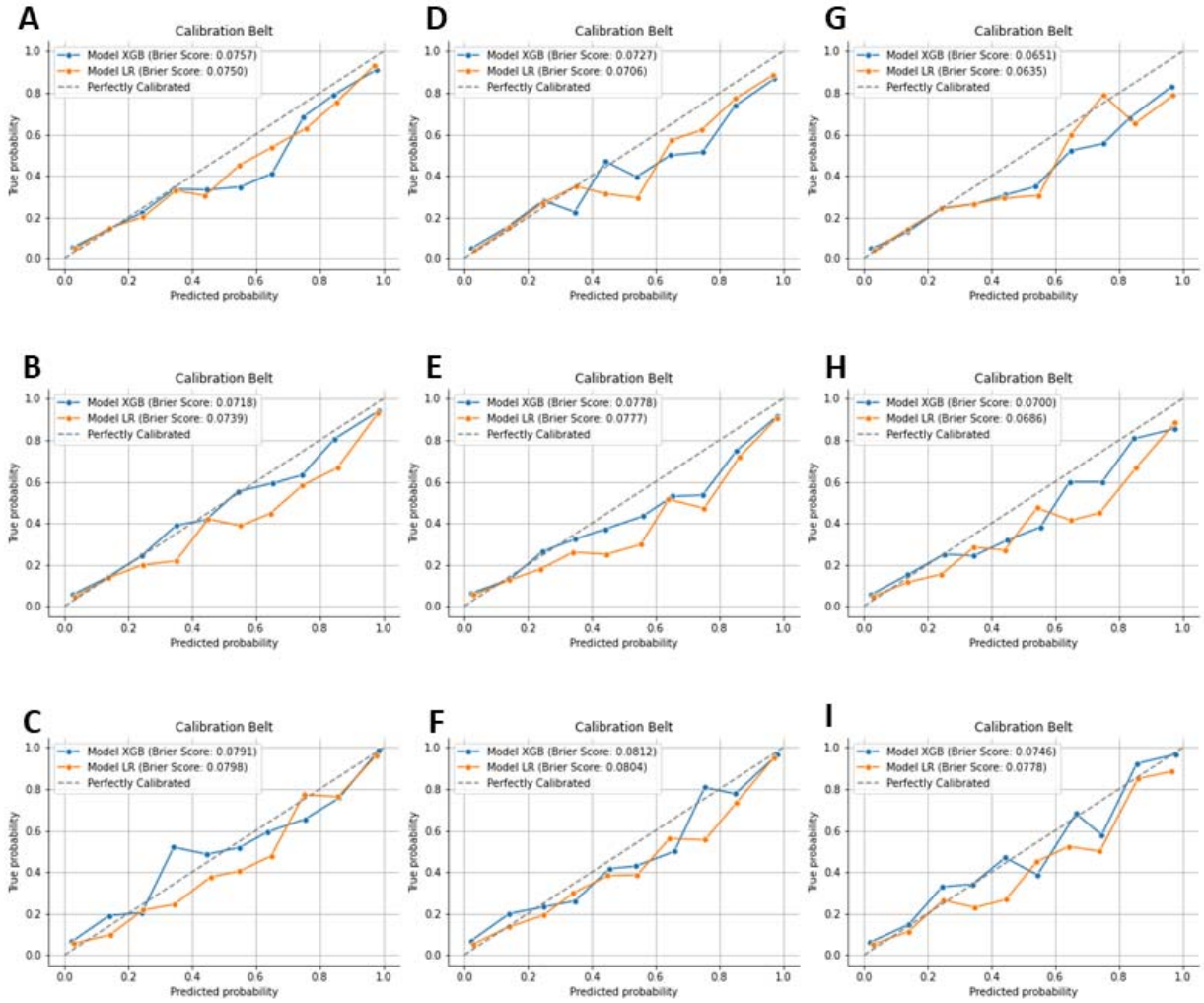

Supplemental Figure 6. Calibration plots and associated Brier scores for the top performing models for varied time horizons and features windows in the validation dataset. A) 6-hour time horizon and 24-hour feature window; B) 6-hour time horizon and 48-hour feature window; C) 6-hour time horizon and 72-hour feature window; D) 12-hour time horizon and 24-hour feature window; E) 12-hour time horizon and 48-hour feature window; F) 12-hour time horizon and 72-hour feature window; G) 24-hour time horizon and 24-hour feature window; H) 24-hour time horizon and 48-hour feature window; I) 24-hour time horizon and 72-hour feature window. Abbreviations: LR, logistic regression; XGB, extreme gradient boosted.

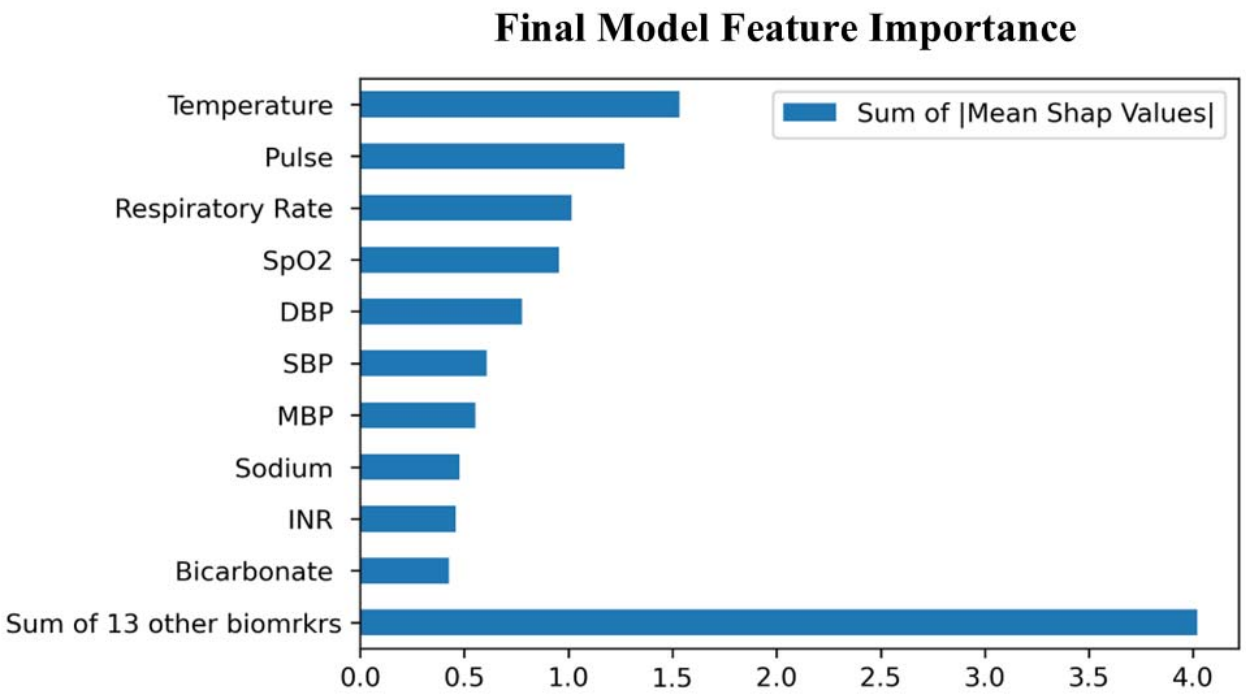

Supplemental Figure 7. Top 10 biomarker feature categories based on Shap values for the 12-hour time horizon 48-hour feature window XGBoost model from the development site. Each category contains several features, e.g. Temperature contains maximum temperature, minimum temperature, average temperature, etc. The blue bars represent the sum of the mean Shap values for each category. Abbreviations: biomrkrs, biomarkers.

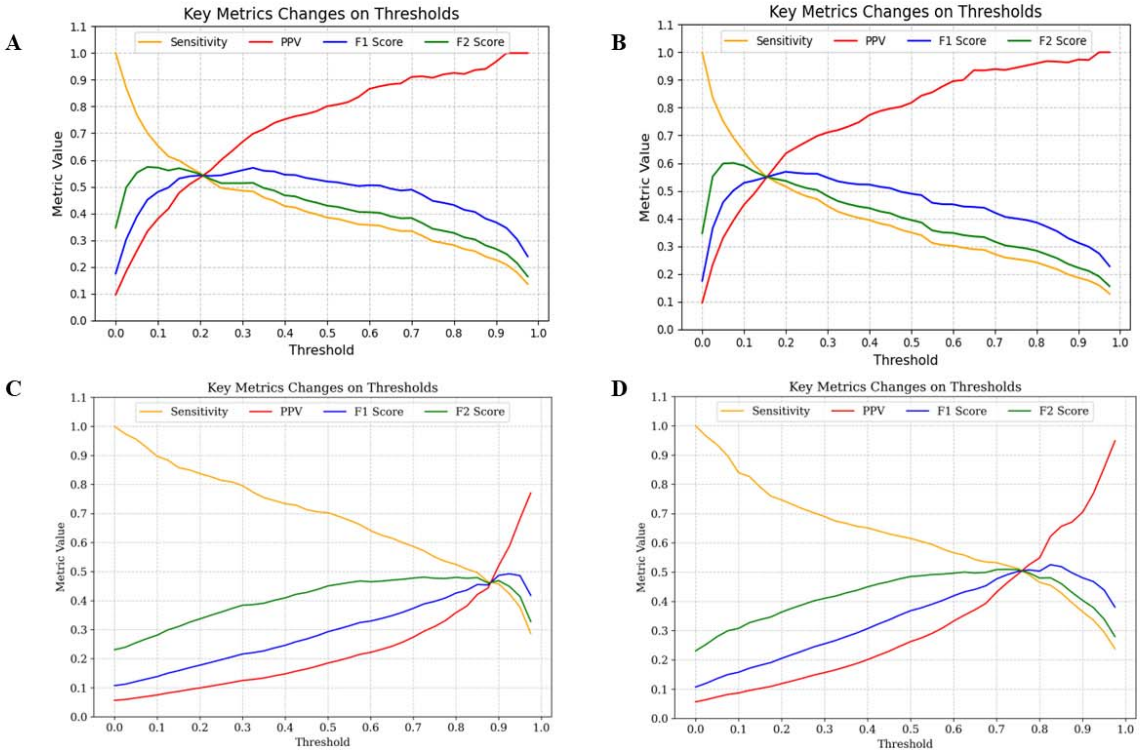

Supplemental Figure 8. Plots the key statistical performance metrics sensitivity (gold line), positive predictive value (PPV, red line), F1 score (blue line), and F2 score (green line) with metric values on the y-axis and model output thresholds on the x-axis for the generalizable A) logistic regression model in the development site test dataset; B) extreme gradient boosting model in the development site test data set; C) logistic regression model in the external validation dataset; D) extreme gradient boosting model in the external validation site dataset.

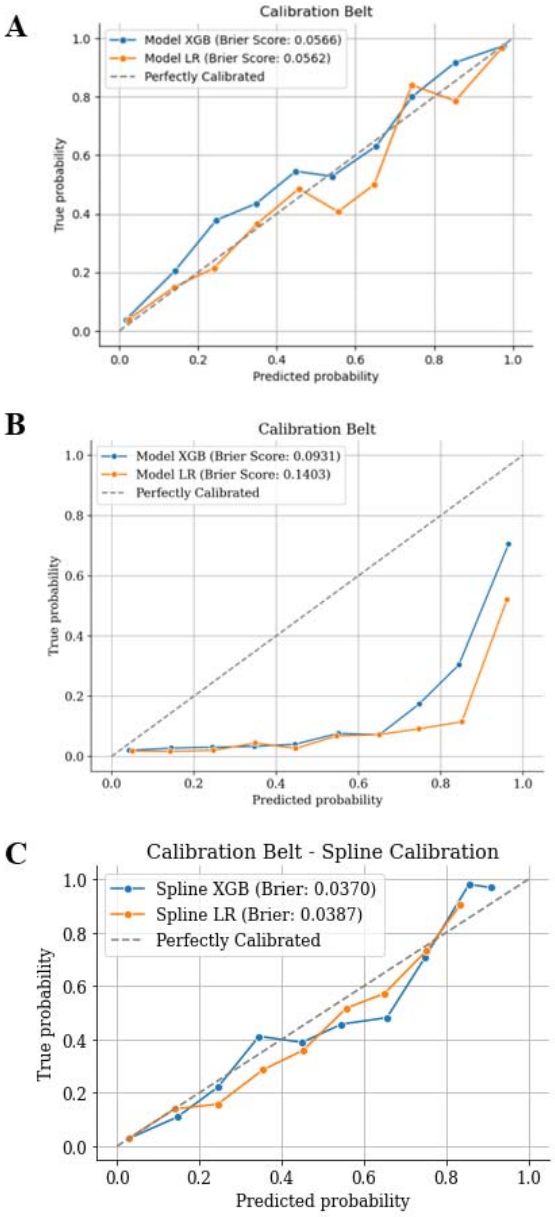

Supplemental Figure 9. Calibration plots for the generalizable model in the A) development site test dataset, B) the external validation site dataset, and C) the external validation site dataset after spline recalibration.

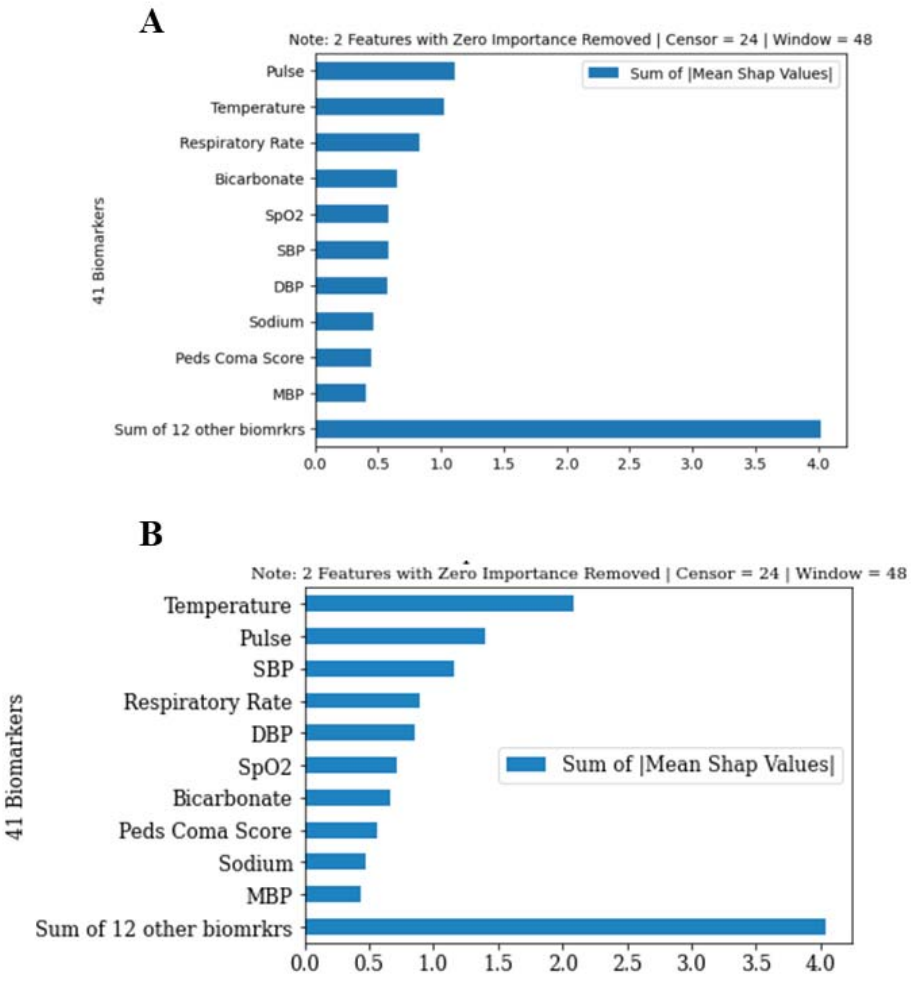

Supplemental Figure 10. Feature importance analysis for the generalizable model in the A) development site test dataset and B) external validation site dataset.